[36] Laughner E, Taghavi P, Chiles K, Mahon PC, Semenza GL. HER2 (neu) signaling increases the rate of hypoxia-inducible factor 1alpha (HIF-1alpha) synthesis: novel mechanism for HIF-1-mediated vascular endothelial growth factor expression. Mol Cell 2001;21:3995–4004.

[37] Treins C, Giorgetti-Peraldi S, Murdaca J, Semenza GL, Van Obberghen E. Insulin stimulates hypoxia-inducible factor 1 through a phosphatidylinositol 3-kinase/target of rapamycin-dependent signaling pathway. J Biol Chem 2002;277:27975–81.

[38] Gao N, Ding M, Zheng JZ, Zhang Z, Leonard SS, Liu KJ, et al. Vanadate-induced expression of hypoxia-inducible factor 1 alpha and vascular endothelial growth factor through phosphatidylinositol 3-kinase/Akt pathway and reactive oxygen species. J Biol Chem 2002;277:31963–71.

[39] Funakoshi M, Sonoda Y, Tago K, Tominaga S, Kasahara T. Differential involvement of p38 mitogen-activated protein kinase and phosphatidylinositol 3-kinase in the IL-1-mediated NF-kappa B and AP-1 activation. Int Immunopharmacol 2001;1:595–604.

COMMENTARY

Risk to the coronary arteries of intracoronary stem cell infusion and G-CSF cytokine therapy

Published online March 2, 2004
http://image.thelancet.com/extras/04cmt20web.pdf
See pages 751 and 783

Haemopoietic stem cells that give rise to blood cells and which move between bone marrow and peripheral blood are the best characterised adult stem cells in man. Recent data suggest that adult stem cells generate differentiated cells of a different cell type beyond their own tissue boundaries, a process termed "developmental plasticity". Various stem-cell preparations originating from haemopoietic tissue have been used in in-vivo studies of stem-cell plasticity, including unselected cells from bone marrow, purified haemopoietic stem cells, and single haemopoietic stem cells that originate from either bone marrow or peripheral blood.[1]

Acute myocardial infarction is the most common cause of morbidity and mortality in more developed countries. Therapeutic advances have mainly been targeted at restoring antegrade perfusion in the infarct-related artery. Despite rapid restoration of perfusion, postinfarction heart failure remains a major challenge. A substantial step forward in reversing abnormal cardiac remodelling would be the enhanced generation of cardiac myocytes as well as the stimulation of neovascularisation within the infarcted area. The feasibility of therapeutic angiogenesis by regional implantation of bone marrow-derived mononuclear cells was demonstrated for the first time in patients with chronic limb ischaemia.[2] Thereafter, intracoronary infusion[3,4] or intramyocardial injection[5–7] of bone marrow-derived mononuclear cells or peripheral blood endothelial-like progenitor cells have been shown to be effective in patients with acute myocardial infarction or after myocardial infarction with no other treatment option. Cytokine therapy with granulocyte colony-stimulating factor (G-CSF) improved cardiac function by inducing neovascularisation and myocyte regeneration in mice,[8] whereas myocyte regeneration did not occur in a nonhuman primate model treated with the G-CSF and stem cell factor (SCF) protocol.[9]

Two relevant reports are published in this issue of *The Lancet*. P Richard Vulliet and colleagues show that intracoronary injection of bone marrow-derived mesenchymal stromal cells caused acute myocardial infarction and subacute myocardial microinfarction in a dog model by occluding coronary circulation. These investigators expanded bone marrow-derived mesenchymal stromal cells by cell culture and showed that the size of injected cells was about two-fold larger than freshly prepared nucleated bone marrow cells. In another paper Hyun-Jae Kang and colleagues treated patients who had acute myocardial infarction and who underwent coronary stenting for the culprit lesion of infarction (MAGIC cell trial), with G-CSF and prepared mononuclear cells from their peripheral blood. Intracoronary injection of these cells seemed safe and produced good periprocedural results with improvement of cardiac function and enhanced angiogenesis. G-CSF alone had no effect on cardiac function. These investigators found, however, a mild increase in cardiac enzymes after cell infusion.

The results of these two papers suggest that more investigation of potential complications, such as occlusion of microcoronary circulation, should be done before mesenchymal stromal cells or G-CSF-mobilised cells are routinely injected into the arterial circulation of patients. Kang and colleagues' finding that G-CSF alone showed short-term safety in patients with myocardial infarctions contrasts with a recent report by Hill and colleagues[10] that in 12 patients with intractable angina, the administration of G-CSF was associated with two acute myocardial infarctions and one cardiac death. In that report[10] the enrolled patients were high-risk, with intractable angina and coronary lesions inappropriate for further revascularisation, whereas those enrolled by Kang and colleagues had myocardial infarctions but stable symptoms, and arterial lesions suitable for revascularisation. Since the G-CSF doses used in the two studies were similar, the difference in revascularisation and in the underlying coronary bed may have caused the discrepancy in findings.

Despite the favourable short-term results of infusion of G-CSF-mobilised peripheral blood cells, Kang and colleagues observed an unexpectedly high rate of restenosis. As they discuss, possible explanations for this result include differentiation of G-CSF-mobilised progenitor cells into smooth muscle cells within the stented segment, induction of angiogenesis within the atherosclerotic lesion, and the aggregation of mobilised inflammatory cells within the plaque. This finding is corroborated by several investigators who have reported the induction of acute myocardial infarctions and cerebral infarction in patients after bone marrow transplantation.[11]

Potent angiogenic action of mononuclear cells from peripheral blood not mobilised by G-CSF has been reported in ischaemic myocardium of pigs[12] and human beings[13] and in ischaemic limbs of rats.[14] Intracoronary infusion of normal peripheral-blood-derived mononuclear cells without G-CSF may therefore be feasible as a safer angiogenic cell therapy. Intensive and cautious preclinical studies focusing on the induction of vascular occlusion in atherosclerotic lesions are required to establish the safety and feasibility of G-CSF-mobilised cell infusion therapy. Only if safety is shown should we start multicentre, double-blind clinical trials for such G-CSF cytokine therapy.

I have no conflict of interest to declare.

Hiroaki Matsubara
Department of Cardiovascular Medicine, Kyoto Prefectural University School of Medicine, and Director of Cardiac Stem Cell Project, Translational Research Center, Kyoto University Hospital, Kyoto, Japan
(e-mail: matsubah@koto.kpu-m.ac.jp)

1 Korbling M, Estrov Z. Adult stem cells for tissue repair—new therapeutic concept? *N Engl J Med* 2003; **349:** 570–82.
2 Tateishi-Yuyama E, Matsubara H, Murohara T, et al. Therapeutic angiogenesis for patients with limb ischemia by autologous transplantation of bone marrow cells: a pilot study and a randomised controlled trial. *Lancet* 2002; **360:** 427–35.
3 Strauer BE, Brehm M, Zeus T, et al. Repair of infarcted myocardium by autologous intracoronary mononuclear bone marrow cell transplantation in humans. *Circulation* 2002; **106:** 1913–18.
4 Assmus B, Schachinger V, Teupe C, et al. Transplantation of progenitor cells and regeneration enhancement in acute myocardial infarction (TOPCARE-AMI). *Circulation* 2002; **106:** 3009–17
5 Stamm C, Westphal B, Kleine H-D, et al. Autologous bone-marrow stem-cell transplantation for myocardial regeneration. *Lancet* 2003; **361:** 45–46.
6 Tse H-F, Kwong Y-L, Chan JKF, et al. Angiogenesis in ischaemic myocardium by intramyocardial autologous bone marrow mononuclear cell implantation. *Lancet* 2003; **361:** 47–49.
7 Perin EC, Dohmann HFR, Borojevic R, et al. Transendocardial, autologous bone marrow cell transplantation for severe, chronic ischemic heart failure. *Circulation* 2003; **107:** 2294–2302.
8 Orlic D, Kajstura J, Chimenti S, et al. Mobilized bone marrow cells repair the infarcted heart, improving function and survival. *Proc Natl Acad Sci USA* 2001; **98:** 10344–49.
9 Norol F, Merlet P, Sebillon P, et al. Influence of mobilized stem cells on myocardial infarct repair in a nonhuman primate model. *Blood* 2003; **102:** 4361–68.
10 Hill JM, Paul JD, Powell TM, et al. Efficacy and risk of granulocyte colony stimulating factor administration in patients with severe coronary artery disease. *Circulation* 2003; **108** (supp IV): 478
11 Fukumoto Y, Miyamoto T, Okamura T, et al. Angina pectoris occuring during granulocyte colony-stimulating factor-combined preparatory regimen for autologous peripheral blood stem cell transplantation in a patient with acute myelogenous leukaemia. *Br J Haem* 1997; **97:** 666–68
12 Kamihata H, Matsubara H, Nishiue N, et al. Improvement of collateral perfusion and regional function by catheter-based implantation of peripheral blood mononuclear cells into ischemic hibernating myocardium. *Arterioscler Thromb Vasc Biol* 2002; **22:** 1804–10
13 Inaba S, Egashira K, Kimihiro, et al. Peripheral-blood or bone-marrow mononuclear cells for therapeutic angiogenesis? *Lancet* 2002; **360:** 2083–84.
14 Iba O, Matsubara H, Nozawa Y, et al. Angiogenesis by implantation of peripheral blood mononuclear cells and platelets into ischemic limbs *Circulation* 2002; **106:** 2019–25.

The lessons of MMR

See pages 750 and 820

This week, *The Lancet* prints a partial retraction—a retraction of an interpretation[1]—from the majority of authors of a paper published in February, 1998, by Andrew Wakefield and colleagues.[2] Wakefield and one other co-author, Peter Harvey, have not signed this retraction statement. We hope to publish their response very shortly. The original report[2] made clear that the authors "did not prove an association" between measles, mumps, and rubella (MMR) vaccine and a newly described syndrome of bowel disease and autism. But the authors did raise the possibility of a link, on the basis of parental and medical histories, and they suggested that "further investigations are needed to examine this syndrome and its possible relation to this vaccine". This interpretation of their data, together with a suggestion made by Wakefield during a separate press conference held at the Royal Free Hospital that there was a case for splitting the MMR vaccine into its component parts, triggered a collapse in confidence in the UK's MMR vaccination programme. It is the interpretation expressed about a connection between the vaccine and the new syndrome that is now being retracted. Today's retraction comes after debate following the release of new information 2 weeks ago about the circumstances surrounding the publication of this work.[3] An enormous amount of effort has gone into reviewing and analysing the events before and after publication of the 1998 article. It is now time to look forward.

Autism research

In 1943, Leo Kanner described 11 children with a condition that differed "markedly and uniquely from anything reported so far".[4] He believed that the characteristics of these children, the fundamental feature of whom was their "inability to relate themselves in the ordinary way to people and situations from the beginning of life", constituted a syndrome, one that he described as "an extreme autistic aloneness". The recognition of such a distinct clinical entity was important, even urgent at that time. Kanner described how several of the children who had been introduced to him were inappropriately labelled as "idiots or imbeciles". One lived in a "state school for the feebleminded, and two had been previously considered as schizophrenic".

Since Kanner's report, autism and autism-like conditions have become common diagnoses[5] and exercise much media attention.[6] There is a strong underlying genetic basis to autism. But the idea of a "late-onset" variant[7] raised a possibility that there might be psychological and organic factors contributing to autism's cause and course. One unexpected consequence of the debate surrounding MMR has been a redirection of public attention to a condition that has often been neglected by medicine. In a review of the epidemiology and causes of autism, for example, the UK's Medical Research Council (MRC) summarised existing knowledge and identified strategic themes deserving further investigation (panel).[8] There are large and surprising gaps in our knowledge of a condition that affects as many as 6 per 1000 young children.

The UK Government announced a further £2·75 million of new and ring-fenced money for autism research in 2002. The first funding decisions by the MRC are expected in May this year. The MRC is strongly committed to autism research, presently funding seven research projects at a cost of over £4 million. To make the best of what are still limited

Future strategic themes in autism research[8]

- Case definition
  Improving phenotypic identification
- Epidemiological frameworks
  Pinpointing environmental and genetic influences
- Integrated research strategies
  Developing a comprehensive neurosciences approach
- Hypotheses about abnormal physiology
  Requiring experimental rigour and independent replication
- Research capacity and the service interface
  Promoting collaboration, career development, and child-care and support service expansion
- Lay participation
  Strengthening research networks through partnership

Aldosterone Directly Induces Myocyte Apoptosis Through Calcineurin-Dependent Pathways

Akiko Mano, MD; Tetsuya Tatsumi, MD, PhD; Jun Shiraishi, MD, PhD; Natsuya Keira, MD, PhD; Tetsuya Nomura, MD; Mitsuo Takeda, MD; Susumu Nishikawa, MD; Satoshi Yamanaka, MD, PhD; Satoaki Matoba, MD, PhD; Miyuki Kobara, MD, PhD; Hideo Tanaka, MD, PhD; Takeshi Shirayama, MD, PhD; Tetsuo Takamatsu, MD, PhD; Yoshihisa Nozawa, PhD; Hiroaki Matsubara, MD, PhD

Background—Aldosterone has recently attracted considerable attention for its involvement in the pathophysiology of heart failure, in which apoptotic cell loss plays a critical role. This study examined whether aldosterone directly induces myocyte apoptosis via its specific receptors.

Methods and Results—Neonatal rat cardiac myocytes were exposed to aldosterone (10^{-8} to 10^{-5} mol/L). Nuclear staining with Hoechst 33258 showed that aldosterone induced myocyte apoptosis in a dose- and time-dependent fashion. Treatment of myocytes with 10^{-5} mol/L aldosterone significantly increased the percentage of apoptosis (15.5±1.4%) compared with serum-deprived control (7.3±0.6%). Radio ligand binding assay revealed the existence of plasma membrane receptor with high affinity (K_d, 0.2 nmol/L) for aldosterone in cardiac myocytes but not in fibroblasts. Aldosterone rapidly (≈30 seconds) mobilized $[Ca^{2+}]_i$ that was blocked by neomycin. Aldosterone induced dephosphorylation of the proapoptotic protein Bad, enhancement of mitochondrial permeability transition, decrease in mitochondrial membrane potential, and release of cytochrome c from the mitochondria into the cytosol with concomitant activation of caspase-3. These effects of aldosterone were inhibited by concurrent treatment with either an L-type Ca^{2+} channel antagonist, nifedipine, or inhibitors for the Ca^{2+}-dependent phosphatase calcineurin, cyclosporin A and FK506.

Conclusions—The present study demonstrates for the first time that the specific plasma membrane receptor (coupled with phospholipase C) for aldosterone is present on cardiac myocytes and that aldosterone accelerates the mitochondrial apoptotic pathway through activation of calcineurin and dephosphorylation of Bad, suggesting that the proapoptotic action of aldosterone may directly contribute to the progression of heart failure. **(*Circulation*. 2004;110:317-323.)**

Key Words: angiotensin ■ apoptosis ■ heart failure

Heart failure is a common, lethal condition associated with various cardiovascular diseases and remains a major cause of morbidity and mortality worldwide.[1] Cardiac myocytes are known to undergo apoptosis in some pathological conditions, such as hypoxia and ischemia-reperfusion.[2,3] Moreover, recent studies provide direct evidence that the progressive loss of cardiac myocytes by apoptosis is one of the most important components in the pathogenesis of heart failure.[4]

Several lines of evidence suggest that neurohormonal mechanisms play a central role in the progression of heart failure.[5] In addition to activation of the sympathetic nervous system, the renin-angiotensin-aldosterone system is known to have a deleterious effect on the heart. Recent studies report that aldosterone is produced in failing human hearts[6] and that aldosterone receptor antagonists, such as spironolactone and eplerenone, dramatically reduce morbidity and mortality from heart failure.[7,8] Aldosterone-mediated nongenomic action, such as rapid activation of protein kinase C and rise in $[Ca^{2+}]_i$ associated with phosphoinositide hydrolysis, is demonstrated in vascular smooth muscle cells (VSMCs) and endothelial cells.[9,10] However, it remains to be determined whether a specific plasma membrane receptor is present on cardiac myocytes.

Aldosterone-mediated action may cause various intracellular responses associated with elevation of $[Ca^{2+}]_i$. Recent studies have suggested that elevation of $[Ca^{2+}]_i$ induces apoptosis in some types of cells by activation of calcineurin, a Ca^{2+}-dependent phosphatase.[11] Because calcineurin affects the function of the proapoptotic protein Bad, which accelerates the mitochondrial death signaling pathway,[11] we hypothesized that aldosterone can directly induce myocyte apoptosis by activation of calcineurin.

This study was designed to determine whether cardiac myocytes have a plasma membrane receptor specific for aldosterone and whether aldosterone-mediated nongenomic

Received January 21, 2004; revision received April 1, 2004; accepted April 5, 2004.

From the Departments of Cardiovascular Medicine and Pathology and Cell Regulation (H.T., T.T.), Kyoto Prefectural University School of Medicine, Kyoto, and Pharmacobioregulation Research Laboratory (Y.N.), Taiho Pharmaceutical Co. Ltd, Iinou, Japan.

Correspondence to Tetsuya Tatsumi, MD, PhD, Department of Cardiovascular Medicine, Kyoto Prefectural University School of Medicine, Kawaramachi-Hirokoji, Kamigyo-ku, Kyoto 602-8566, Japan. E-mail tatsumi@koto.kpu-m.ac.jp

Circulation is available at http://www.circulationaha.org

DOI: 10.1161/01.CIR.0000135599.33787.CA

signaling affects myocyte apoptosis. We found that aldosterone directly induces myocyte apoptosis by activating its membrane receptor-mediated mitochondrial death signaling associated with the calcineurin-Bad pathway.

Methods

Cultured Neonatal Rat Cardiac Myocytes

Primary cultures of neonatal rat cardiac myocytes were prepared from neonatal Wistar rat hearts by digestion with 0.2% collagenase as described previously.[12] All experiments were performed 36 to 48 hours after incubation with DMEM containing 0.5% FBS.

Experimental Protocols

Myocytes were incubated with aldosterone (10^{-8} to 10^{-5} mol/L) for 24 hours or incubated with 10^{-5} mol/L aldosterone for the indicated periods (12 to 48 hours). To evaluate the effects of Ca^{2+} and calcineurin, myocytes were stimulated by 10^{-5} mol/L aldosterone for 24 hours after pretreatment with nifedipine (10^{-6} mol/L), calcineurin inhibitors, cyclosporin A (10^{-6} mol/L), and FK506 (10 μg/mL) for 1 hour. To examine Bad dephosphorylation, myocytes were incubated with 10^{-5} mol/L aldosterone for 4 hours. Control myocytes were incubated in serum-free DMEM.

Histochemical Determination of Apoptosis

Histochemical staining of myocytes was performed.[2] The cells were visualized by fluorescein microscopy, and the images were generated by dual-exposure photography. Apoptotic cells were identified on the basis of distinctive condensed or fragmented nuclear morphology, and apoptotic cell counts were expressed as a percentage of the total number of nuclei counted.[12]

Radioligand Binding Assay

Membrane fraction of myocytes and fibroblasts were prepared as previously described.[12,13] The fraction (50 μg of protein) was incubated for 1 hour at 37°C in a assay buffer. [1,2-^{3}H] aldosterone (Amersham, UK), specific activity of 39.8 Ci/mmol, was added at concentrations from 0.01 to 10 nmol/L. Incubates were transferred to Whatman GF/C filters (Whatman), and radioactivity was measured in a liquid scintillation counter. Specific binding was determined experimentally from the difference between counts in the absence and presence of 10 μmol/L cold unlabeled aldosterone. The *Kd* and Bmax values were estimated by Scatchard analysis of the saturation data.

Intracellular Ca^{2+} Levels

Determination of $[Ca^{2+}]_i$ was performed as previously described.[10] Myocytes grown on glass base dishes were loaded with 2×10^{-6} mol/L fura-2 AM (Molecular Probes) for 1 hour at 37°C. Then myocytes were incubated with PBS and $[Ca^{2+}]_i$ images were visualized using Ion Optix dual-wavelength imaging system. Integration time was 0.017 seconds at each wavelength (340 and 380 nm), with a time increment of 0.1 seconds. The autofluorescence level was subtracted from each reading before calculation of $[Ca^{2+}]_i$. The system was calibrated by the method of Grynkiewicz et al.[14]

Mitochondrial Permeability Transition and Transmembrane Potential

Myocytes were loaded with 5×10^{-6} mol/L calcein-acetoxymethylester (calcein-AM, Molecular Probes) in the presence of 2 to 5×10^{-3} mol/L cobalt chloride to quench the cytoplasmic signals.[15] Then fluorescent intensities of the myocytes were determined. Loss of $\Delta\psi_m$ was assessed by Dye JC-1.[16] Cells grown on coverslips were incubated in PBS containing 10^{-5} mol/L JC-1 at 37°C for 5 minutes. Fluorescence emission at 527 and 590 nm was determined after excitation at 480 nm.

Immunoblotting

Antibodies for cytochrome c (7H8.2C12, PharMingen), Bad (Transduction Laboratories), phospho-Bad (Cell Signaling), and horseradish peroxidase–conjugated anti-IgG (Amersham) were used, and immunoblotting was performed as described.[12,13,17] Chemoluminescence was detected with ECL Western blot detection kits (Amersham).

Caspase-3 Activity

Caspase-3 enzymatic activity was determined with a CPP32 assay kit (MBL), which detects the production of the chromophore p-nitroanilide after its cleavage from the peptide substrate DEVD-p-nitroanilide, as described previously.[18]

Statistical Analysis

Data are expressed as mean±SE of at least 6 samples derived from more than 6 separate experiments. Skewed data (see Figure 3) were expressed as median (interquartile range). Differences were analyzed by 1-way ANOVA combined with the Bonferroni test. $P<0.05$ was considered to indicate statistical significance.

Results

Induction of Myocyte Apoptosis

Histochemical nuclear staining with Hoechst 33258 and immunohistochemical staining of cellular desmin showed that aldosterone increased apoptotic myocytes in a dose-dependent fashion (Figure 1A). Treatment of myocytes with 10^{-6} mol/L and 10^{-5} mol/L aldosterone significantly increased the percentage of myocyte apoptosis to 12.3% and 15.5%, respectively, compared with serum-deprived control (7.3%) (Figure 1B). Aldosterone 10^{-5} mol/L also increased apoptotic myocytes in a time-dependent fashion (Figures 1A and 1C). We also assessed the percentage of myocyte apoptosis by fluorescence-activated cell sorter analysis and ascertained that the percentage of apoptosis was almost compatible with that estimated by Hoechst 33258 staining (data not shown).[13] Treatment of myocytes with 10^{-5} mol/L aldosterone for 48 hours did not increase necrotic cell death as estimated by calcein acetoxymethyl ester and ethidium homodimer-1 staining or creatine kinase activity in the medium (data not shown).

Aldosterone Receptor on Plasma Membrane of Cardiac Myocytes

Specific saturable binding of aldosterone to plasma membranes of myocytes is illustrated in Figure 2. Scatchard analysis of specific binding in plasma membrane fraction shows maximum binding of 10.3±0.4 fmol/mg protein, with a calculated *Kd* of 0.23±0.03 nmol/L. In contrast, no specific binding sites for aldosterone were detected in plasma membrane fraction from cardiac fibroblasts.

Intracellular Ca^{2+} Mobilization

Figure 3 illustrates the rapid induction of $[Ca^{2+}]_i$ by aldosterone in myocytes. Myocytes treated with aldosterone under Ca^{2+}-free conditions showed a rapid increase in fluorescence intensity reflecting the mobilization of $[Ca^{2+}]_i$ (Figure 3A). This phenomenon began within 30 seconds after addition and then slowly reached a plateau after 60 seconds. The median increase of $[Ca^{2+}]_i$ induced by aldosterone was 147 nmol/L (67 to 282 nmol/L) (Figure 3B). Neomycin, an inhibitor of

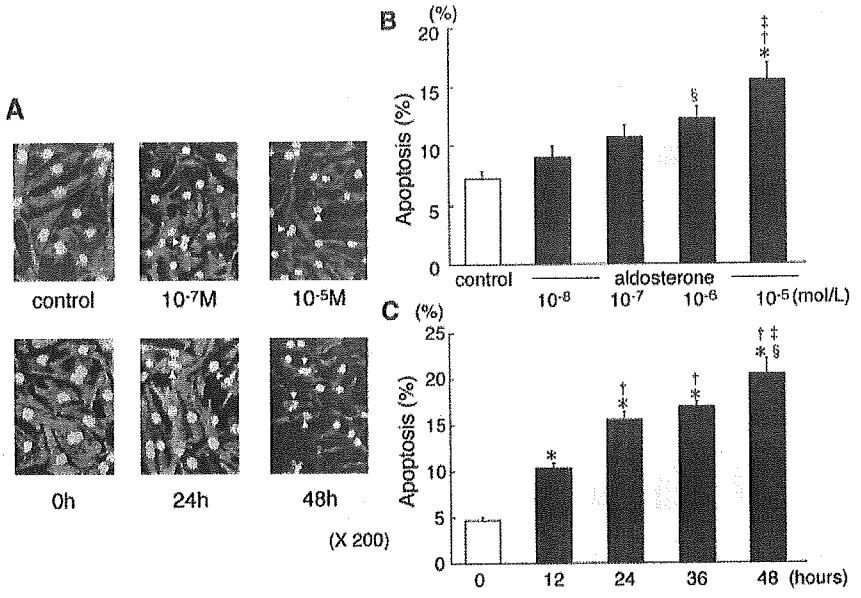

Figure 1. Aldosterone-induced myocyte apoptosis. A, Myocytes were treated with the indicated concentration of aldosterone for the indicated time periods. The myocytes were then stained with an anti-desmin polyclonal antibody and Hoechst 33258 (magnification ×200). Arrows indicate the typical feature of apoptotic myocytes. B, Dose dependency of aldosterone-induced myocyte apoptosis. Myocytes were treated with the indicated concentration of aldosterone (10^{-8} to 10^{-5} mol/L) for 24 hours. The percentage of apoptotic cells was calculated as described in Methods (n=6). *P<0.0001, §P<0.001 vs control; †P<0.0001 vs 10^{-8} mol/L; ‡P<0.01 vs 10^{-7} mol/L. C, Time course of aldosterone-induced myocyte apoptosis. Myocytes were treated with 10^{-5} mol/L aldosterone for the indicated time periods. The percentage of apoptotic cells was calculated as described in Methods (n=6). *P<0.0001 vs 0 hours; †P<0.0001 vs 12 hours; §P<0.001 vs 24 hours; ‡P<0.01 vs 36 hours.

phospholipase C, completely blocked this rapid effect of aldosterone (Figure 3C).

Effects of Ca^{2+} Antagonist and Calcineurin Inhibitors

Treatment of myocytes with aldosterone markedly increased apoptosis (2.2-fold), as estimated on the basis of nuclear morphology (Figure 4). When myocytes were pretreated with nifedipine, cyclosporin A, or FK506, the percentage of apoptotic myocytes was significantly (P<0.0001) decreased. Treatment of myocytes with nifedipine, cyclosporin A, or FK506 alone did not affect the percentage of apoptosis (data not shown). Cell length determined directly from the images using an edge-detection system[19] was decreased (43% to 48%, P<0.001, n=6) by addition of nifedipine (10^{-8} to 10^{-6} mol/L) but not cyclosporin A (10^{-6} mol/L) or FK506 (10 μg/mL), suggesting that contractile inhibition by Ca^{2+} channel antagonist or addition of calcineurin inhibitors is not involved in the cell survival.

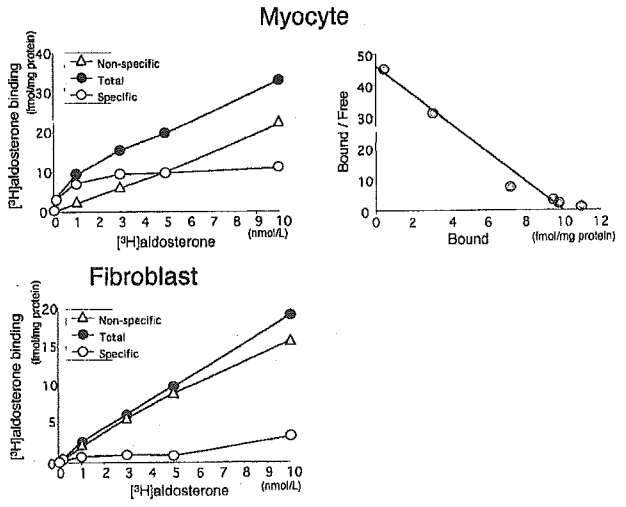

Figure 2. Binding of [^{3}H] aldosterone to cardiac myocytes and fibroblasts. Total, specific, and nonspecific binding of [^{3}H] aldosterone (0.01 to 10 nmol/L) to the membrane fractions of the myocytes (top left) and fibroblasts (bottom left) was examined. Representative tracings are shown from 4 independent experiments. ●, total binding; ○, specific binding; △, nonspecific binding. Scatchard analysis of the specific binding is performed in myocytes (top right).

Dephosphorylation of Bad

In the serum-deprived control, Bad consistently existed in highly phosphorylated form in the myocytes, whereas aldosterone markedly inhibited the Bad phosphorylation levels to 31% of the control and increased the dephosphorylation levels of Bad to 198% (Figure 5). This effect was maximum at 4 hours and then gradually decreased (data not shown). When myocytes were pretreated with nifedipine, cyclosporin A, or FK 506, dephosphorylation levels of Bad were substantially inhibited toward the control level.

Mitochondrial Permeability Transition, Membrane Potential, and Cytochrome C Release

Myocytes displayed punctate green-staining mitochondria, indicative of an intact mitochondrial membrane under control conditions. When myocytes were treated with aldosterone for 24 hours, green fluorescence in mitochondria was markedly reduced, consistent with permeability transition (PT) pore opening (Figure 6A, top). Pretreatment of myocytes with nifedipine, cyclosporin A, or FK506 significantly inhibited the loss of green fluorescence in mitochondria and thus prevented aldosterone-induced PT pore opening.

Myocytes showed red-orange mitochondrial staining by JC-1, indicative of normal high membrane potentials under control conditions.[20] In contrast, myocytes treated with aldosterone showed green fluorescence, indicating loss of $\Delta\psi_m$ (Figure 6A, bottom). Myocytes pretreated with nifedipine, cyclosporin A, or FK506 showed increased red-fluorescent intensity, indicating that $\Delta\psi_m$ was markedly preserved.

As shown in Figure 6, cytochrome c was detected only in the mitochondrial fraction under control conditions. Aldosterone inhibited the immunoreactivity of cytochrome c in

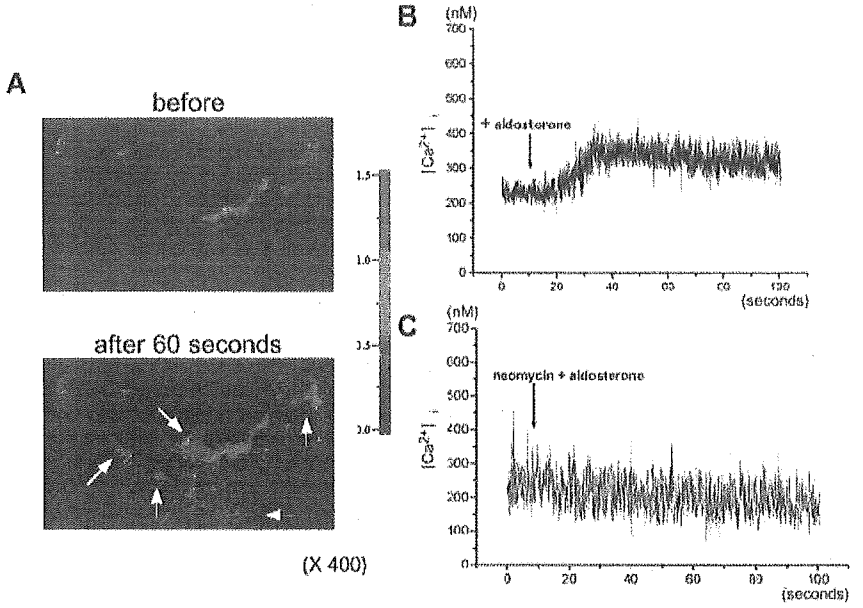

Figure 3. Calcium images and time course changes of $[Ca^{2+}]_i$ in myocytes. Myocytes were loaded with 2×10^{-6} mol/L fura-2 AM for 1 hour, and $[Ca^{2+}]_i$ was measured by dual-wavelength fluorescence of fura-2 in a microscopic cell-imaging system. A, Representative images (magnification ×400) of the myocytes are shown before and 60 seconds after addition of aldosterone (10^{-5} mol/L). Arrows show the myocytes with increased fluorescence intensity. B, Time course changes of $[Ca^{2+}]_i$ in the myocytes were measured before and after addition of aldosterone (10^{-5} mol/L). C, After pretreatment with neomycin (3×10^{-4} mol/L) for 15 minutes, myocytes were stimulated by aldosterone (10^{-5} mol/L), and $[Ca^{2+}]_i$ was determined. Tracings shown are representative from 5 independent experiments.

mitochondria to 36% of the control, whereas the activity in the cytosolic fraction was increased up to 395% of the control, which was inhibited by pretreatment with nifedipine, cyclosporin A, or FK506.

Activation of Caspase-3

Caspase-3 activity in the myocytes treated with aldosterone for 24 hours significantly increased by 1.4-fold compared with the serum-deprived control (Figure 7). Pretreatment with nifedipine, cyclosporin A, or FK506 inhibited the aldosterone-induced activation of caspase-3 to 1.1-fold, 1.1-fold, and 1.0-fold, respectively.

Discussion

The present study demonstrates for the first time that (1) aldosterone directly induces myocyte apoptosis in a dose- and time-dependent fashion; (2) plasma membrane receptor with high-affinity binding sites for aldosterone exists on cardiac myocytes but not cardiac fibroblasts; (3) aldosterone rapidly increases $[Ca^{2+}]_i$ associated with phospholipase C hydrolysis and induces dephosphorylation of Bad with enhancement of mitochondrial PT, decrease in $\Delta\psi_m$, release of cytochrome c from the mitochondria into the cytosol, and activation of caspase-3; and (4) aldosterone-mediated effects are inhibited by nifedipine, cyclosporin A, or FK506. Thus, our data clearly demonstrate that aldosterone induces a nongenomic intracellular response through phosphoinositide hydrolysis, resulting in stimulation of mitochondrial apoptotic pathway associated with calcineurin signaling and dephosphorylation of Bad.

In addition to the classic adrenal biosynthetic pathway, previous clinical and experimental studies have demonstrated the production of aldosterone and the presence of mineralocorticoid receptor in cardiovascular tissue.[21–23] Recent studies provide evidence that aldosterone rapidly increases $[Ca^{2+}]_i$ in endothelial cells and VSMCs by prompting transport of Ca^{2+}

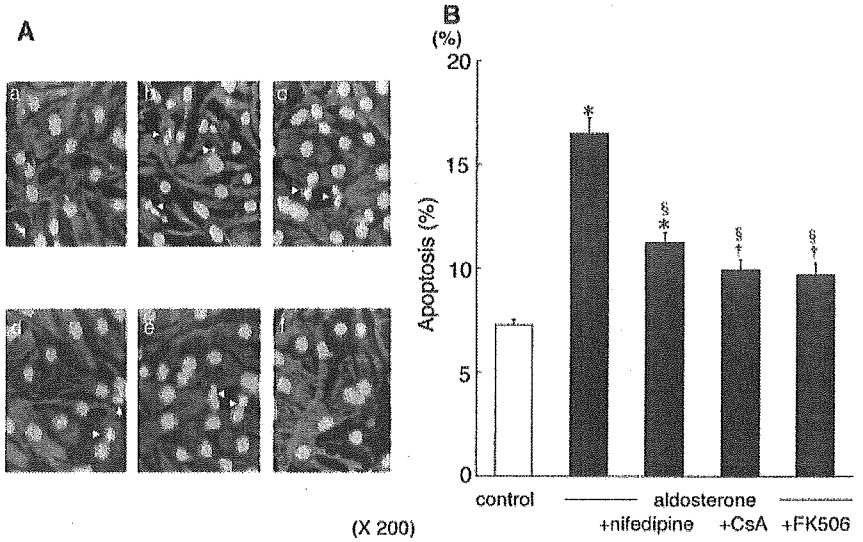

Figure 4. Histochemical characterization of apoptotic myocytes. After pretreatment with nifedipine (10^{-6} mol/L), cyclosporin A (CsA) (10^{-6} mol/L), or FK506 (10 μg/mL) for 1 hour, myocytes were stimulated by aldosterone (10^{-5} mol/L) for 24 hours. Myocytes were stained with an anti-desmin polyclonal antibody and Hoechst 33258. A, Representative micrographs (magnification ×200). a, control; b, aldosterone; c, aldosterone+nifedipine; d, aldosterone+CsA; e, aldosterone+FK506; f, CsA alone. B, Percentage of apoptotic myocytes. Myocyte apoptosis was calculated as described in Methods (n=6). *P<0.0001, †P<0.001 vs control; §P<0.0001 vs aldosterone.

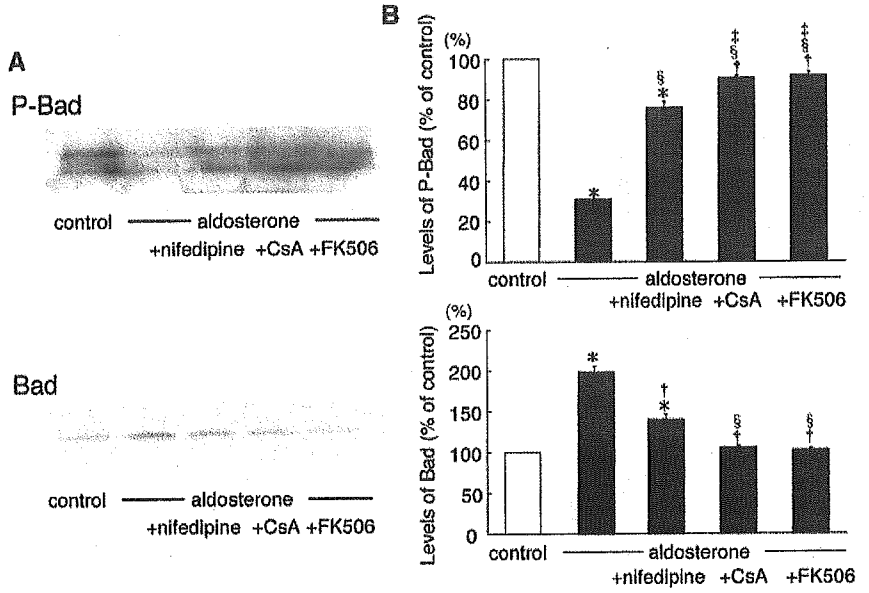

Figure 5. Western blot analysis of Bad. After pretreatment with nifedipine (10^{-6} mol/L), CsA (10^{-6} mol/L), or FK506 (10 μg/mL) for 1 hour, myocytes were stimulated by aldosterone (10^{-5} mol/L) for 4 hours. Cell extracts (55 μg protein) were probed with anti-phospho(P)-Bad or anti-Bad antibodies. A, Immunoblots shown are representative from 3 independent experiments. B, Densitometric analysis for dephosphorylation of Bad. Levels of P-Bad (top) and Bad (bottom) are shown as a percentage of change in the mean value derived from 3 independent experiments. Top, $^*P<0.0001$, $\dagger P<0.01$ vs control; $\S P<0.0001$ vs aldosterone; $\ddagger P<0.0001$ vs aldosterone+nifedipine. Bottom, $^*P<0.0001$ vs control; $\dagger P<0.0001$ vs aldosterone; $\S P<0.001$ vs aldosterone+nifedipine.

from storage sites via activation of phospholipase C, followed by an increase in inositol-1,4,5-triphosphate.[9,10] Such aldosterone-mediated nongenomic action was not observed in isolated adult rat cardiac myocytes; Benitah and Vassort[24] reported that Ca^{2+} current was increased by long-term incubation but not during short-term incubation (up to 6 hours) of aldosterone. This discrepancy between cardiac myocytes and VSMCs suggested that nongenomic aldosterone effects are restricted to specific target tissues. The present study showed for the first time the existence of the plasma membrane receptor specific for aldosterone in cardiac myocytes but not in cardiac fibroblasts, the binding affinity of which was very similar to that already reported in membrane fractions from human mononuclear leukocytes and pig kidneys (*K*d, 0.23 nmol/L vs 0.1 to 0.4 nmol/L, respectively).[9] Furthermore, we found that nuclear fractions from myocytes have specific binding sites for aldosterone, with maximum binding of 504 fmol/mg protein and *K*d of 1.2 nmol/L, suggesting that myocardial plasma membrane receptor is apparently different from intracellular receptor. Taken together, these data clearly indicate that cardiac myocytes and VSMCs possess a similar membrane receptor for aldosterone that is coupled with phospholipase C and that its activation leads to a rapid intracellular signaling cascade associated with $[Ca^{2+}]_i$ and protein kinase C.

Apoptosis is governed by families of proteins with positive and negative regulatory members acting at serial steps along a programmed pathway.[25] Bad is usually maintained in phosphorylated and sequestered form in the cytosol by 14-3-3 proteins and cannot exert its death-promotive action. However, when Bad is dephosphorylated by apoptotic signals, it heterodimerizes with Bcl-2 and Bcl-xL and suppresses their survival signals.[26] Recently, Ca^{2+}-mobilizing agents have been reported to dephosphorylate Bad by activating calcineurin and to augment Bad heterodimerization with Bcl-xL, leading to apoptosis.[11] In the present study, we have clearly shown that aldosterone decreases the phosphorylation levels of Bad and that this effect was significantly inhibited when myocytes were pretreated with an L-type Ca^{2+} channel antagonist or calcineurin inhibitors. Our findings therefore strongly suggest that Ca^{2+}-dependent calcineurin activation and dephosphorylation of Bad have a central role in the aldosterone-induced death-signaling pathway.

Mitochondria possesses the porin channel, called voltage-dependent-anion channel, in the outer membrane.[27] Binding of Bcl-xL protein to this channel usually closes (stabilizes) the PT pore. However, when Bad migrates into mitochondria and heterodimerizes with Bcl-xL, voltage-dependent-anion channel is opened. Thus, Bad increases mitochondrial PT and releases cytochrome c into the cytosol, with concomitant loss of $\Delta\psi_m$.[11,27] In our study, aldosterone induced PT pore opening, loss of $\Delta\psi_m$, release of cytochrome c into the cytosol, and activation of caspase-3, which were inhibited by concurrent treatment with nifedipine, cyclosporin A, or FK506. These findings indicate that aldosterone accelerates the mitochondrial apoptotic pathway triggered by calcineurin-induced dephosphorylation of Bad.

The level of aldosterone in plasma is approximately 10^{-7} mol/L in patients with heart failure, and the level of aldosterone in myocardium is approximately 17 times higher than that in plasma.[28,29] The aldosterone concentrations used in our study are therefore considered clinically relevant. Campbell et al[30] reported in aldosterone-treated rats that aldosterone caused myocyte necrosis by mitochondrial injury and sarcomeric contraction, because an increase in circulating aldosterone concentrations caused electrolyte imbalance, such as an enhanced potassium excretion, leading to activation of Na^+/H^+ and Na^+/Ca^{2+} exchange in cardiac mitochondria and sarcolemma. Taken together, in the in vivo situation in which the circulating aldosterone levels and electrolyte homeostasis are maintained, aldosterone may induce myocyte apoptosis rather than necrosis.

The present data indicate that nifedipine significantly inhibits the proapoptotic effect of aldosterone, suggesting that transsarcolemmal Ca^{2+} influx is also involved in aldosterone-induced increase in $[Ca^{2+}]_i$. Indeed, Benitah and Vassort[24]

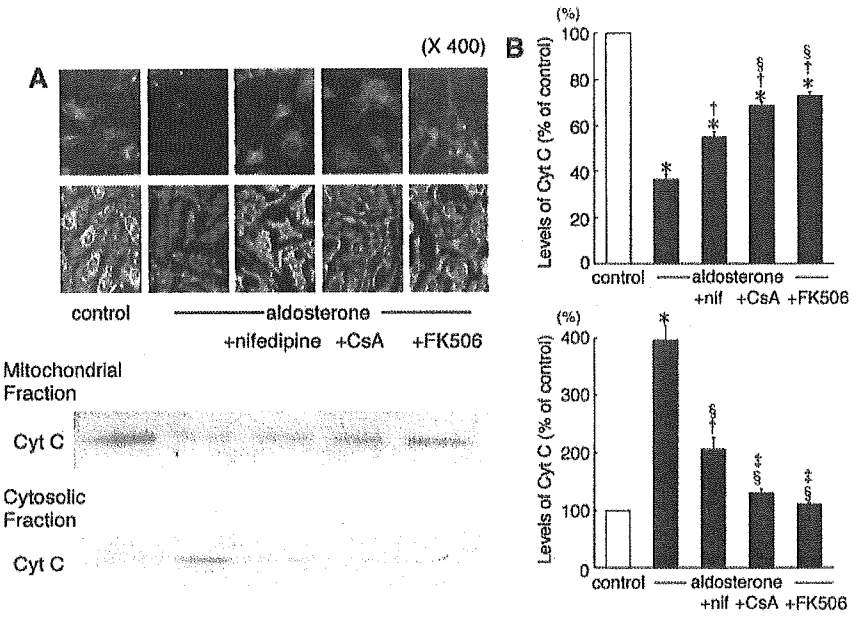

Figure 6. Changes of mitochondrial permeability transition, loss of mitochondrial transmembrane potential ($\Delta\psi_m$), and translocation of cytochrome c (Cyt C). A, Myocytes were stimulated by aldosterone (10^{-5} mol/L) for 24 hours after preincubation with nifedipine (10^{-6} mol/L), CsA (10^{-6} mol/L), or FK506 (10 μg/mL) for 1 hour. Mitochondrial PT and $\Delta\psi_m$ of the myocytes were monitored with calcein-AM and JC-1. Mitochondrial and cytosolic fractions (20 μg protein) were probed with antibody for Cyt C. Representative immunoblots are shown from 3 independent experiments. B, Densitometric analysis of Cyt C release. Levels of Cyt C are shown as a percentage of change in the mean values from 3 independent experiments compared with serum-deprived control. Top (mitochondrial fraction), *$P<0.0001$ vs control; †$P<0.0001$ vs aldosterone; §$P<0.001$ vs aldosterone+nifedipine (nif). Bottom (cytosolic fraction), *$P<0.0001$, †$P<0.001$ versus control; §$P<0.0001$ vs aldosterone; ‡$P<0.01$ vs aldosterone+nif.

have reported that aldosterone upregulates transsarcolemmal Ca^{2+} current into myocytes, probably by stimulating L-type Ca^{2+} channel subunit mRNA expression. Concurrent treatment of the myocytes with actinomycin D, an inhibitor of transcription, or cycloheximide, an inhibitor of protein synthesis, blunted the aldosterone-induced apoptosis (data not shown), therefore indicating that an L-type Ca^{2+} channel activation through a genomic effect is also partly involved in the effect of aldosterone. Thus, this evidence strongly supports the findings that calcineurin inhibitors were more effective than nifedipine in suppressing the proapoptotic effect of aldosterone.

In conclusion, our study has demonstrated that cardiac myocytes possess a plasma membrane receptor specific for aldosterone coupled with phospholipase C and that aldosterone induces myocyte apoptosis through a calcineurin-dependent mitochondrial death-signaling pathway triggered by rapid increase in intracellular Ca^{2+} levels. Aldosterone thus plays a crucial role in the progression of heart failure, and regulation of calcineurin and Bcl-2 family proteins may have important implications for the development of new therapeutic strategies for patients with heart failure.

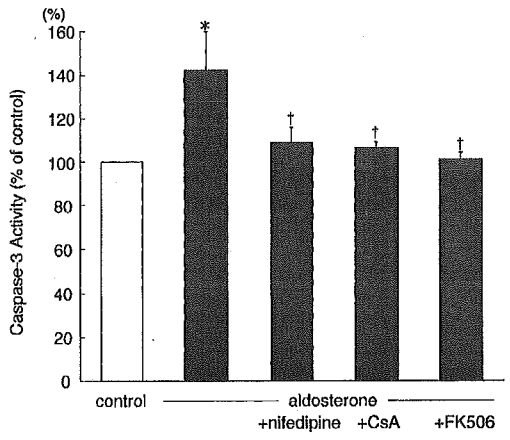

Figure 7. Caspase-3 activity in myocytes. Myocytes were subjected to pretreatment with nifedipine (10^{-6} mol/L), CsA (10^{-6} mol/L), or FK506 (10 μg/mL) for 1 hour, followed by aldosterone (10^{-5} mol/L) stimulation for 24 hours. Caspase-3 activity was determined as described in Methods. Activation level of caspase-3 is shown as a percentage of change in mean values of 6 samples derived from at least 3 separate experiments. *$P<0.001$ vs control, †$P<0.01$ vs aldosterone.

Acknowledgments

This study was supported in part by Grants-in-Aid from the Ministry of Education, Science and Culture and from the Ministry of Health Labor and Welfare, Japan.

References

1. Braunwald E, Bristow MR. Congestive heart failure: fifty years of progress. *Circulation.* 2000;102:IV14–IV23.
2. Tatsumi T, Shiraishi J, Keira N, et al. Intracellular ATP is required for mitochondrial apoptotic pathways in isolated hypoxic rat cardiac myocytes. *Cardiovasc Res.* 2003;59:428–440.
3. Fliss H, Gattinger D. Apoptosis in ischemic and reperfused rat myocardium. *Circ Res.* 1996;79:949–956.
4. Narula J, Haider N, Virmani R, et al. Apoptosis in myocytes in end-stage heart failure. *N Engl J Med.* 1996;335:1182–1189.
5. Packer M. The neurohormonal hypothesis: a theory to explain the mechanism of disease progression in heart failure. *J Am Coll Cardiol.* 1992;20:248–254.
6. Mizuno Y, Yoshimura M, Yasue H, et al. Aldosterone production is activated in the failing ventricles in human. *Circulation.* 2001;103:72–77.
7. Pitt B, Zannad F, Remme WJ, et al. The effect of spironolactone on morbidity and mortality in patients with severe heart failure: Randomized Aldactone Evaluation Study Investigators. *N Engl J Med.* 1999;341:709–717.
8. Pitt B, Remme W, Zannad F, et al. Eplerenone, a selective aldosterone blocker, in patients with left ventricular dysfunction after myocardial infarction. *N Engl J Med.* 2003;348:1309–1321.
9. Falkenstein E, Tillmann HC, Christ M, et al. Multiple actions of steroid hormones: a focus on rapid, nongenomic effects. *Pharmacol Rev.* 2000;52:513–556.
10. Wehling M, Neylon CB, Fullerton M, et al. Nongenomic effects of aldosterone on intracellular Ca^{2+} in vascular smooth muscle cells. *Circ Res.* 1995;76:973–979.
11. Wang HG, Pathan N, Ethell IM, et al. Ca^{2+}-induced apoptosis through calcineurin dephosphorylation of BAD. *Science.* 1999;284:339–343.

12. Shiraishi J, Tatsumi T, Keira N, et al. Important role of energy-dependent mitochondrial pathways in cultured rat cardiac myocyte apoptosis. *Am J Physiol Heart Circ Physiol.* 2001;281:H1637–H1647.
13. Yamanaka S, Tatsumi T, Shiraishi J, et al. Amlodipine inhibits doxorubicin-induced apoptosis in neonatal rat cardiac myocytes. *J Am Coll Cardiol.* 2003;41:870–878.
14. Grynkiewicz G, Poenie M, Tsien RY. A new generation of Ca^{2+} indicators with greatly improved fluorescence properties. *J Biol Chem.* 1985; 260:3440–3450.
15. Petronilli V, Miotto G, Canton M, et al. Imaging the mitochondrial permeability transition pore in intact cells. *Biofactors.* 1998;8:263–272.
16. Ankarcrona M, Dypbukt JM, Bonfoco E, et al. Glutamate-induced neuronal death: a succession of necrosis or apoptosis depending on mitochondrial function. *Neuron.* 1995;15:961–973.
17. Yang J, Liu X, Bhalla K, et al. Prevention of apoptosis by Bcl-2: release of cytochrome c from mitochondria blocked. *Science.* 1997;275: 1129–1132.
18. Casciola-Rosen L, Nicholson DW, Chong T, et al. Apopain/CPP32 cleaves proteins that are essential for cellular repair: a fundamental principle of apoptotic death. *J Exp Med.* 1996;183:1957–1964.
19. Tatsumi T, Matoba S, Kawahara A, et al. Cytokine-induced nitric oxide production inhibits mitochondrial energy production and impairs contractile function in rat cardiac myocytes. *J Am Coll Cardiol.* 2000;35: 1338–1346.
20. Cook SA, Sugden PH, Clerk A. Regulation of bcl-2 family proteins during development and in response to oxidative stress in cardiac myocytes: association with changes in mitochondrial membrane potential. *Circ Res.* 1999;85:940–949.
21. Slight SH, Joseph J, Ganjam VK, et al. Extra-adrenal mineralocorticoids and cardiovascular tissue. *J Mol Cell Cardiol.* 1999;31:1175–1184.
22. Harada E, Yoshimura M, Yasue H, et al. Aldosterone induces angiotensin-converting-enzyme gene expression in cultured neonatal rat cardiocytes. *Circulation.* 2001;104:137–139.
23. Lombes M, Oblin ME, Gasc JM, et al. Immunohistochemical and biochemical evidence for a cardiovascular mineralocorticoid receptor. *Circ Res.* 1992;71:503–510.
24. Benitah JP, Vassort G. Aldosterone upregulates Ca^{2+} current in adult rat cardiomyocytes. *Circ Res.* 1999;85:1139–1145.
25. Oltvani ZN, Korsmeyer SJ. Checkpoints of dueling dimers foli death wishes. *Cell.* 1994;79:189–192.
26. Zha J, Harada H, Yang E, et al. Serine phosphorylation of death agonist BAD in response to survival factor results in binding to 14–3–3 not Bcl-X(L). *Cell.* 1996;87:619–628.
27. Shimizu S, Narita M, Tsujimoto Y. Bcl-2 family proteins regulate the release of apoptogenic cytochrome c by the mitochondrial channel VDAC. *Nature.* 1999;399:483–487.
28. Rousseau MF, Gurne O, Duprez D, et al. Beneficial neurohormonal profile of spironolactone in severe congestive heart failure: results from the RALES neurohormonal substudy. *J Am Coll Cardiol.* 2002;40: 1596–1601.
29. Silvestre JS, Robert V, Heymes C, et al. Myocardial production of aldosterone and corticosterone in the rat: physiological regulation. *J Biol Chem.* 1998;273:4883–4891.
30. Campbell SE, Janicki JS, Matsubara BB, et al. Myocardial fibrosis in the rat with mineralocorticoid excess. *Am J Hypertens.* 1993;6:487–495.

Autologous Bone-Marrow Mononuclear Cell Implantation Improves Endothelium-Dependent Vasodilation in Patients With Limb Ischemia

Yukihito Higashi, MD; Masashi Kimura, MD; Keiko Hara, MD; Kensuke Noma, MD; Daisuke Jitsuiki, MD; Keigo Nakagawa, MD; Tetsuya Oshima, MD; Kazuaki Chayama, MD; Taijiro Sueda, MD; Chikara Goto, RTP, MS; Hiroaki Matsubara, MD; Toyoaki Murohara, MD; Masao Yoshizumi, MD

Background—Patients with limb ischemia were associated with endothelial dysfunction. The purpose of this study was to determine whether autologous bone-marrow mononuclear cell (BM-MNC) implantation improves endothelial dysfunction in patients with limb ischemia.

Methods and Results—We evaluated the leg blood flow (LBF) response to acetylcholine (ACh), an endothelium-dependent vasodilator, and sodium nitroprusside (SNP), an endothelium-independent vasodilator, before and after BM-MNC implantation in 7 patients with limb ischemia. LBF was measured with a mercury-filled Silastic strain-gauge plethysmograph. The number of BM-MNCs implanted into ischemic limbs was $1.6\times10^9\pm0.3\times10^9$. The number of $CD34^+$ cells included in the implanted BM-MNCs was $3.8\times10^7\pm1.6\times10^7$. BM-MNC implantation improved the ankle-brachial pressure index (0.33 ± 0.21 to 0.39 ± 0.17, $P=0.06$), transcutaneous oxygen pressure (28.4 ± 11.5 to 36.6 ± 5.2 mm Hg, $P=0.03$), and pain-free walking time (0.8 ± 0.6 to 2.9 ± 2.2 minutes, $P=0.02$). After BM-MNC implantation, LBF response to ACh was enhanced (19.3 ± 6.8 versus 29.6 ± 7.1 mL/min per 100 mL; $P=0.002$). The vasodilatory effect of SNP was similar before and after BM-MNC implantation.

Conclusions—These findings suggest that BM-MNC implantation augments endothelium-dependent vasodilation in patients with limb ischemia. ***(Circulation.* 2004;109:1215-1218.)**

Key Words: angiogenesis ■ cells ■ endothelium ■ ischemia

Recent studies have shown that bone-marrow mononuclear cell (BM-MNC) implantation increases collateral vessel formation in both ischemic limb models and patients with limb ischemia.[1,2] However, it is not clear whether these collateral arteries have normal vascular function, especially endothelial function. Endothelial dysfunction is the initial step in the pathogenesis of atherosclerosis and plays an important role in development and maintenance of atherosclerosis.[3] Limb ischemia is generally associated with endothelial dysfunction.[4,5] Therefore, it is clinically important to evaluate the vascular function of collateral arteries induced by BM-MNC implantation. We hypothesized that BM-MNC implantation would improve impaired endothelial function in patients with limb ischemia.

To determine the effect of BM-MNC implantation on endothelial function in patients with limb ischemia, we evaluated endothelium-dependent vasodilation induced by acetylcholine (ACh) and endothelium-independent vasodilation induced by sodium nitroprusside (SNP) before and after BM-MNC implantation.

Methods

Subjects

Seven patients with peripheral arterial disease (6 men and 1 woman; mean age, 64 ± 9 years) who had rest pain and nonhealing ulcers and who were not candidates for angioplasty or surgical revascularization were enrolled in this study. The diagnosis of limb ischemia was confirmed by angiography. Patients with diabetes mellitus, coronary artery disease, and history of malignant disorders were excluded. Four of the 7 patients had smoking habits, and those 4 patients stopped smoking 2 months before BM-MNC implantation. The drugs used were not changed throughout the study. Lifestyle also was regulated throughout the study. The study protocol was approved by the Ethics Committee of the Hiroshima University Graduate School of Medicine. Written informed consent for participation was obtained from all subjects.

Received March 5, 2003; de novo received December 15, 2003; revision received January 28, 2003; accepted January 28, 2003.

From the Department of Cardiovascular Physiology and Medicine (Y.H., M.Y.), Department of Medicine and Molecular Science (M.K., K.H., K. Noma, D.J., K. Nakagawa, K.C.), Division of Physical Therapy, Institute of Health Sciences (C.G.), and the Department of Clinical Laboratory Medicine (T.O.), Department of Surgery (T.S.), Hiroshima University Graduate School of Biomedical Sciences, Department of Cardiovascular Medicine (H.M.), Kyoto Prefectural University of Medicine, and Department of Cardiology (T.M.), Nagoya University Graduate School of Medicine.

Correspondence to Yukihito Higashi, MD, PhD, FAHA, Department of Cardiovascular Physiology and Medicine, Graduate School of Biomedical Sciences, Hiroshima University, 1-2-3 Kasumi, Minami-ku, Hiroshima 734-8551, Japan. E-mail yhigashi@hiroshima-u.ac.jp

Circulation is available at http://www.circulationaha.org

DOI: 10.1161/01.CIR.0000121427.53291.78

Patient	Age, y	Sex	Disorders	Drugs	BM-MNC Count, No. of Cells	CD34 (+) Cells in BM-MNC	ABI	TcO_2, mm Hg	Pain-Free Walking, min	Basal LBF mL · min^{-1} · 100 mL^{-1}
Patient 1										
Before	74	Male	HL	CaB, statin, APA	1.8×10^9	2.5×10^7	0.35	36	0.91	1.3
After 4 wk							0.44	41	1.22	2.4
After 24 wk							0.41	40	1.35	2.3
Patient 2										
Before	62	Male	HL	Statin	1.4×10^9	3.3×10^7	0.60	42	2.14	3.5
After 4 wk							0.62	45	6.89	3.9
After 24 wk							...	...	...	...
Patient 3										
Before	73	Male	HT, HL	CaB, ACEI, APA	1.6×10^9	4.2×10^7	0.23	25	1.21	2.2
After 4 wk							0.21	31	3.35	2.1
After 24 wk							0.22	32	2.98	2.2
Patient 4										
Before	56	Male	None	APA	2.2×10^9	6.2×10^7	ND	9	0	0.2
After 4 wk							0.26	37	2.34	0.6
After 24 wk							0.28	33	2.99	0.6
Patient 5										
Before	73	Female	HT	CaB, APA	1.5×10^9	1.3×10^7	0.39	38	0.56	1.9
After 4 wk							0.40	37	1.63	3.8
After 24 wk							0.38	36	1.35	3.2
Patient 6										
Before	51	Male	HL	Statin, APA	1.4×10^9	3.9×10^7	0.19	20	0.33	0.3
After 4 wk							0.22	31	0.98	0.3
After 24 wk							0.21	29	1.01	0.3
Patient 7										
Before	59	Male	HT	CaB, APA	1.2×10^9	5.1×10^7	0.52	29	0.76	2.6
After 4 wk							0.61	34	4.75	3.3
After 24 wk							0.59	32	5.11	3.1

ABI indicates ankle-brachial pressure index; TcO_2, transcutaneous oxygen; HL, hyperlipidemia; HT, hypertension; CaB, calcium blocker; APA, antiplatelet agent; ACEI, angiotensin-converting enzyme inhibitor; and ND, not detected.

BM-MNC Implantation

BM-MNCs were sorted and implanted in patients with limb ischemia as previously described.[2]

Effect of BM-MNC Implantation on Endothelial Function in Patients With Limb Ischemia

Leg vascular responses to ACh (Daiichi Pharmaceutical Co) and SNP (Maluishi Pharmaceutical Co) were evaluated by use of a mercury-filled Silastic strain-gauge plethysmograph (EC-5R, D.E. Hokanson, Inc) before and at 4 weeks after BM-MNC implantation in all subjects and at 24 weeks after BM-MNC implantation in 6 of the 7 subjects. Subjects fasted for at least 12 hours before cell implantation. They were kept in the supine position in a quiet, dark, air-conditioned room (temperature, 22°C to 25°C) throughout the study. A 23-gauge polyethylene catheter was inserted into the BM-MNC–implanted femoral artery for the infusion of ACh and SNP under local anesthesia. After each patient had spent 30 minutes in the supine position, we measured leg blood flow (LBF) and arterial blood pressure. Then, the effects of the ACh and SNP infusion on leg hemodynamics were measured. ACh (7.5, 15, and 30 μg/min) and SNP (0.75, 1.5, and 3.0 μg/min) were infused intra-arterially for 5 minutes at each dose. The infusions of ACh and SNP were performed in random order. Each study proceeded after the LBF had returned to baseline.

To evaluate the drug-related effect on endothelium-dependent vasodilation, the infusion of ACh and SNP was performed using a protocol identical to that used for the study of limb ischemic patients with implanted MN-MNCs before and after 4 weeks of follow-up in 5 patients with limb ischemia (4 men and 1 woman; mean age, 65±7 years) as a control group. Five patients were taking ACE inhibitors and antiplatelet agents; 3 of those 5 patients were taking calcium antagonists, and 2 were taking statins. The patients were subjected to 4 weeks of follow-up without any drug treatment or lifestyle modification.

Measurement of LBF

The blood flow was measured using a mercury-filled Silastic strain-gauge plethysmograph (EC-5R, D.E. Hokanson, Inc) as previously described.[6,7]

Statistical Analysis

Results are presented as the mean±SD. All reported probability values were 2-tailed. Values of $P<0.05$ were considered significant. Comparisons of parameters before and after BM-MNC implantation were performed with adjusted means by ANCOVA using baseline data as covariates. Comparisons of time-course curves of parameters during the infusions of ACh and SNP were analyzed by 2-way ANOVA for repeated measures on 1 factor followed by the Bonferroni correction for multiple-paired comparisons.

Results

Clinical Characteristics

The baseline clinical characteristics before and at 4 weeks and 24 weeks after BM-MNC implantation of patients with limb ischemia are summarized in the Table. The number of BM-MNCs implanted into ischemic limbs was $1.6\times10^9\pm0.3\times10^9$. The number of $CD34^+$ cells included in the implanted BM-MNCs was $3.8\times10^7\pm1.6\times10^7$. BM-MNC implantation improved the ankle-brachial pressure index from 0.33 ± 0.21 to 0.39 ± 0.17 after 4 weeks ($P=0.06$) and to 0.35 ± 0.38 after 24 weeks ($P=0.16$), transcutaneous oxygen pressure from 28.4 ± 11.5 to 36.6 ± 5.2 mm Hg after 4 weeks ($P=0.03$) and to 33.7 ± 3.8 mm Hg after 24 weeks ($P=0.06$), pain-free walking time from 0.8 ± 0.6 to 2.9 ± 2.2 minutes after 4 weeks ($P=0.02$) and to 2.5 ± 1.6 minutes after 24 weeks ($P=0.03$), and basal LBF from 1.7 ± 1.2 to 2.4 ± 1.4 mL/min per 100 mL tissue after 4 weeks ($P=0.04$) and to 2.0 ± 1.2 mL/min per 100 mL tissue after 24 weeks ($P=0.05$).

BM-NMC implantation did not alter blood pressures (mean blood pressure, from 86.2 ± 10.3 to 88.1 ± 11.2 mm Hg after 4 weeks and to 87.3 ± 12.1 mm Hg after 24 weeks) or serum concentrations of total cholesterol (from 5.28 ± 1.24 to 5.22 ± 1.06 mmol/L after 4 weeks and to 5.23 ± 1.18 mmol/L after 24 weeks), LDL cholesterol (from 3.88 ± 0.78 to 3.78 ± 0.72 mmol/L after 4 weeks and to 3.72 ± 0.81 mmol/L after 24 weeks), glucose (from 4.6 ± 0.4 to 4.5 ± 0.5 mmol/L after 4 weeks and to 4.6 ± 0.6 mmol/L after 24 weeks), and insulin (from 41.8 ± 9.8 to 42.3 ± 10.1 pmol/L after 4 weeks and to 43.6 ± 11.4 pmol/L after 24 weeks).

Effect of BM-MNC Implantation on Endothelial Function in Patients With Limb Ischemia

The intra-arterial infusion of ACh increased LBF in a dose-dependent manner. After BM-MNC implantation, LBF responses to ACh were enhanced in patients with limb ischemia (Figure, top). There was no significant difference in LBF response to ACh after 4 weeks and 24 weeks of follow-up (Figure, top). The intra-arterial infusion of SNP also increased LBF in a dose-dependent manner. The LBF response to SNP was unaffected by BM-MNC implantation (Figure, bottom). In the control group, there was no significant difference in LBF responses to ACh and SNP before and those after 4 weeks and 24 weeks of follow-up (Figure). No significant change was observed in arterial blood pressure or heart rate in response to intra-arterial infusion of either ACh or SNP before or after BM-MNC implantation and after 4 weeks of follow-up.

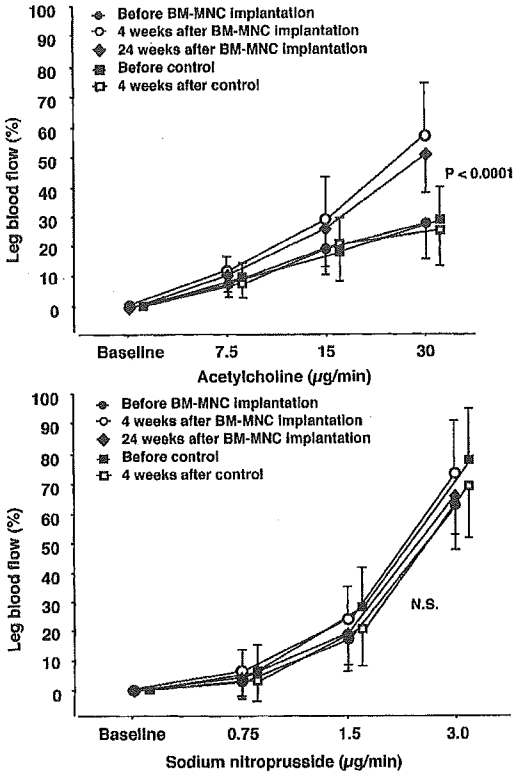

Comparison of LBF (as % change from basal flow) response to ACh administration (top) and SNP administration (bottom) before and after BM-NMC implantation of 4 weeks and 24 weeks of follow-up in patients with limb ischemia.

Discussion

In the present study, BM-MNC implantation improved not only limb ischemic symptoms and findings of angiography but also endothelium-dependent vasodilation in patients with limb ischemia. This beneficial effect of BM-MNC implantation on vascular function may be selective in endothelium-dependent vasodilation (endothelial cell function) but not in endothelium-independent vasodilation (smooth muscle cell function).

Our results showed that BM-MNC implantation increased the ankle-brachial pressure index, transcutaneous oxygen pressure, and basal LBF per se. Therefore, one possible mechanism by which BM-MNC implantation augments endothelium-dependent vasodilation is by increasing shear stress results from blood flow. Acute or chronic increases in shear stress stimulate the release of nitric oxide in isolated vessels and cultured cells through the enhanced expression of endothelial nitric oxide synthase gene.[8,9]

BM-MNCs ($CD34^+$ fraction) include endothelial progenitor cells and various angiogenetic growth factors, such as the vascular endothelial growth factor (VEGF) and angiopoietin families. Supplementation of the progenitor endothelial cells results in augmentation of neovascularization of ischemic tissue and repair of mature endothelial cells that release nitric oxide.[10] VEGF induces the formation of collateral vessels and increases collateral blood flow, leading to improvement in endothelium-dependent vasodilation.[11] In addition, VEGF directly upregulates endothelial nitric oxide synthase expression and increases subsequent nitric oxide release.[12] Rajagopalan et al[5] recently reported that gene therapy using an adenoviral vector encoding a 121-amino-acid isoform of VEGF augmented ACh-induced vasodilation in lower-leg circulation in patients with peripheral arterial disease. Although the mechanism by which BM-MNC implantation improves endothelial function in patients with limb ischemia is not clear, the multiplier effect of progenitor endothelial cells and VEGF may contribute to the angiogenesis-induced improvement in endothelium-dependent vasodilation.

We have recently shown that antihypertensive agents, such as ACE inhibitors, restore endothelial function in patients with mild to moderate hypertension but not in patients with severe hypertension.[13] It is clinically important that endothelial dysfunction is reversible by BM-MNC implantation in patients with severe atherosclerosis. BM-MNC implantation is expected to prevent the development of atherosclerosis through improvement in endothelial function.

Although a drastic change in endothelial function was observed after BM-MNC implantation, the number of subjects in this study was small, and the observation period is relatively short. In addition, this phase 1 clinical trial was not placebo-controlled. Controlled studies using a large population of patients and with long observation periods are needed to determine the role of BM-MNC implantation in endothelial function in patients with severe atherosclerosis.

Although the effectiveness of therapeutic angiogenesis with VEGF gene therapy in patients with peripheral arterial diseases has been established, BM-MNC implantation therapy may provide a new aspect of therapeutic angiogenesis in such patients.

References

1. Shintani S, Murohara T, Ikeda H, et al. Augmentation of postnatal neovascularization with autologous bone marrow transplantation. *Circulation*. 2001;103:897–895.
2. Tateishi-Yuyama E, Matsubara H, Murohara T, et al. Therapeutic angiogenesis for patients with limb ischaemia by autologous transplantation of bone-marrow cells: a pilot study and a randomized controlled trial. *Lancet*. 2002;360:427–435.
3. Ross R. The pathogenesis of atherosclerosis. *N Engl J Med*. 1999;340: 115–126.
4. Boger RH, Bode-Boger SM, Brandes R, et al. Biochemical evidence for impaired nitric oxide synthase in patients with peripheral arterial occlusive disease. *Circulation*. 1997;95:2068–2074.
5. Rajagopalan S, Shah M, Luciano A, et al. Adenovirus-mediated gene transfer of $VEGF_{121}$ improves lower-extremity endothelial function and flow reserve. *Circulation*. 2001;104:753–755.
6. Panza JA, Quyyumi AA, Brush JE Jr, et al. Abnormal endothelium-dependent vascular relaxation in patients with essential hypertension. *N Engl J Med*. 1990;323:22–27.
7. Higashi Y, Sasaki S, Nakagawa K, et al. Endothelial function and oxidative stress in renovascular hypertension. *N Engl J Med*. 2002;346: 1954–1962.
8. Miller VM, Vanhoutte PM. Enhanced release of endothelium-derived factors by chronic increases in blood flow. *Am J Physiol*. 1988;255: H446–H451.
9. Uematsu M, Ohara Y, Navas JP, et al. Regulation of endothelial cell nitric oxide synthase mRNA expression by shear stress. *Am J Physiol*. 1995; 269:C1371–C1378.
10. Asahara T, Murohara T, Sullivan A, et al. Isolation of putative progenitor endothelial cells for angiogenesis. *Science*. 1997;275:964–967.
11. Bauters C, Asahara T, Zheng LP, et al. Recovery of disturbed endothelium-dependent flow in the collateral-perfused rabbit ischemic hindlimb after administration of vascular endothelial growth factor. *Circulation*. 1995;91:2802–2809.
12. Shen B-Q, Lee DY, Zioncheck TZ. Vascular endothelial growth factor governs endothelial nitric-oxide synthase expression via a KDR/FLK-1 receptor and a protein kinase C signaling pathway. *J Biol Chem*. 1999; 274:33057–33063.
13. Higashi Y, Sasaki S, Nakagawa K, et al. The severity of hypertension affects improved resistance artery endothelial function by angiotensin converting enzyme inhibition. *J Cardiovasc Pharmacol*. 2002;39: 668–676.

Cardiac progenitor cells from adult myocardium: Homing, differentiation, and fusion after infarction

Hidemasa Oh[ab], Steven B. Bradfute[cd], Teresa D. Gallardo[e], Teruya Nakamura[ab], Vinciane Gaussin[f], Yuji Mishina[g], Jennifer Pocius[bh], Lloyd H. Michael[bh], Richard R. Behringer[i], Daniel J. Garry[e], Mark L. Entman[bh], and Michael D. Schneider[abjkl]

[a]Center for Cardiovascular Development, [c]Center for Cell and Gene Therapy, [h]DeBakey Heart Center, and Departments of [b]Medicine, [d]Immunology, [j]Molecular and Cellular Biology, and [k]Molecular Physiology and Biophysics, Baylor College of Medicine, Houston, TX 77030; [e]Department of Medicine, University of Texas Southwestern Medical Center, Dallas, TX 75390; [f]University of Medicine and Dentistry of New Jersey, New Jersey Medical School, Newark, NJ 07103; [g]National Institute of Environmental Health Sciences, Research Triangle Park, NC 27709; and [i]University of Texas M. D. Anderson Cancer Center, Houston, TX 77030

Edited by Eric N. Olson, University of Texas Southwestern Medical Center, Dallas, TX, and approved August 25, 2003 (received for review April 11, 2003)

Potential repair by cell grafting or mobilizing endogenous cells holds particular attraction in heart disease, where the meager capacity for cardiomyocyte proliferation likely contributes to the irreversibility of heart failure. Whether cardiac progenitors exist in adult myocardium itself is unanswered, as is the question whether undifferentiated cardiac precursor cells merely fuse with preexisting myocytes. Here we report the existence of adult heart-derived cardiac progenitor cells expressing stem cell antigen-1. Initially, the cells express neither cardiac structural genes nor *Nkx2.5* but differentiate *in vitro* in response to 5′-azacytidine, in part depending on *Bmpr1a*, a receptor for bone morphogenetic proteins. Given intravenously after ischemia/reperfusion, cardiac stem cell antigen 1 cells home to injured myocardium. By using a Cre/Lox donor/recipient pair (*αMHC-Cre/R26R*), differentiation was shown to occur roughly equally, with and without fusion to host cells.

Cardiomyocytes can be formed, at least *ex vivo*, from diverse adult pluripotent cells (1–5). Apart from therapeutic implications and obviating ethical concerns aroused by embryonic stem cell lines, adult cardiac progenitor cells might provide an explanation distinct from cell cycle reentry, for the reported rare occurrence of cycling ventricular muscle cells (6). However, recent publications suggest the failure of certain stem cells' specification into neurons, skeletal muscle, and myocardium *in vivo* (7, 8) and recommend greater conservatism in evaluating claims of adult stem cell plasticity, for cogent reasons (9–11).

The rarity of cardiogenic conversion by endogenous hematopoietic cells (2, 12), requirements for intracardiac injection (3), or mobilization by cytokines (13), uncertain proof for myocytes of host origin in transplanted human hearts (14), and the confounding possibility of cell fusion after grafting *in vivo* (15, 16) highlight unsettled issues surrounding stem cell plasticity in heart disease. For donor cell types already in clinical studies, the predominant *in vivo* effect of bone marrow or endothelial progenitor cells may be neoangiogenesis, not cardiac specification (17, 18), and skeletal myoblasts, despite integration and survival, are confounded by arrhythmias, perhaps reflecting lack of transdifferentiation (19). These obstacles underscore the need to seek cardiac progenitor cells beyond the few known sources.

Materials and Methods

Flow Cytometry and Magnetic Enrichment. A "total" cardiac population was isolated from 6- to 12-wk-old C57BL/6 mice by coronary perfusion with 0.025% collagenase, as for viable adult mouse cardiomyocytes (20). More typically, a "myocyte-depleted" population was prepared, incubating minced myocardium in 0.1% collagenase (30 min, 37°C), lethal to most adult mouse cardiomyocytes (20). Cells were then filtered through 70-μm mesh. Bone marrow cells (21) were compared, with or without collagenase and filtration. Cells were labeled with stem cell antigen 1 (Sca-1)-phycoerythrin (PE), Sca-1-FITC, c-kit-PE; CD4-, CD8-, B220-, Gr-1-, Mac-1-, TER-119-, CD45-, CD31-, CD38-, and Flk-1-FITC; vascular endothelial-cadherin-biotin; von Willebrand factor-biotin (all Pharmingen); and Flt-1 (Santa Cruz Biotechnology). CD45-PE (Pharmingen) was used for bone marrow cells. Biotinylated antibodies were detected with streptavidin-PE or streptavidin-FITC, Flt-1 with FITC-conjugated secondary antibody (Sigma), and nonviable cells with propidium iodide. Flow cytometry was performed with an EPICS XL-MCL (Beckman Coulter) except as noted. Gates were established by nonspecific Ig binding in each experiment.

Cells labeled with Sca-1-biotin (Pharmingen) were incubated with antibiotin microbeads (Miltenyi Biotec, Auburn, CA) and purified by five to six cycles of magnetic selection (22). Sorted populations were reanalyzed by flow cytometry, and the purity of Sca-1$^+$ cells was confirmed before use.

Gene Expression. RT-PCR primers are available on request. Samples were treated with DNase and assayed in the log-linear range. For expression profiling, RNA was isolated from 5,000 Sca-1$^+$ cells and 5,000 adult cardiomyocytes (Alliance for Cell Signaling, University of Texas Southwestern Medical Center) by using the TriPure Isolation Kit (Roche Applied Science, Indianapolis) and underwent two rounds of amplification. Expression profiling was performed by using Affymetrix (Santa Clara, CA) MG U74Av2 arrays, an Agilent (Palo Alto, CA) GeneArray Scanner, Affymetrix MICROARRAY SUITE, Ver. 5.0, and DCHIP 1.2 (W. Wong, Harvard University, Cambridge, MA).

Cell Culture. Newly isolated cardiac Sca-1$^+$ cells were grown in 35-mm dishes coated with 200 μg/ml fibronectin (Sigma) by using Medium-199/10% FBS, for 3 d (5% CO_2, 37°C). To induce differentiation, cells were cultured in medium containing 2% FBS and 3 μM 5-azacytidine (5-aza; 3 d) (1) or 1% DMSO (1 wk) (23). Cells were photographed by using Zeiss Axioplan 2.

Myocardial Infarction and Cell Delivery. Cell grafting was performed with PKH2-GL dye-labeled cells (24) or a Cre/Lox [*α-myosin heavy chain* (*MHC*)-Cre/*Rosa26 Cre reporter* (*R26R*)] donor/recipient pair (25, 26). The *R26R* reporter line, bearing Cre-dependent *LacZ* behind a loxP-flanked neomycin phosphotransferase (*neo*) stop signal, is transcribed ubiquitously without mosaicism (26), and *αMHC-Cre* mediates efficient recombination at this locus even in early myocardium (25). Ischemia/reperfusion injury was performed in chronically instrumented closed-chest *R26R* mice with an implantable occluder (27). Four

This paper was submitted directly (Track II) to the PNAS office.

Abbreviations: *Bmpr1a*, type IA receptor for bone morphogenetic proteins; MHC, myosin heavy chain; neo, neomycin phosphotransferase; *R26R*, *Rosa26 Cre reporter*; Sca-1, stem cell antigen 1; SP, side population; 5-aza, 5-azacytidine.

[l]To whom correspondence should be addressed. E-mail: michaels@bcm.tmc.edu.

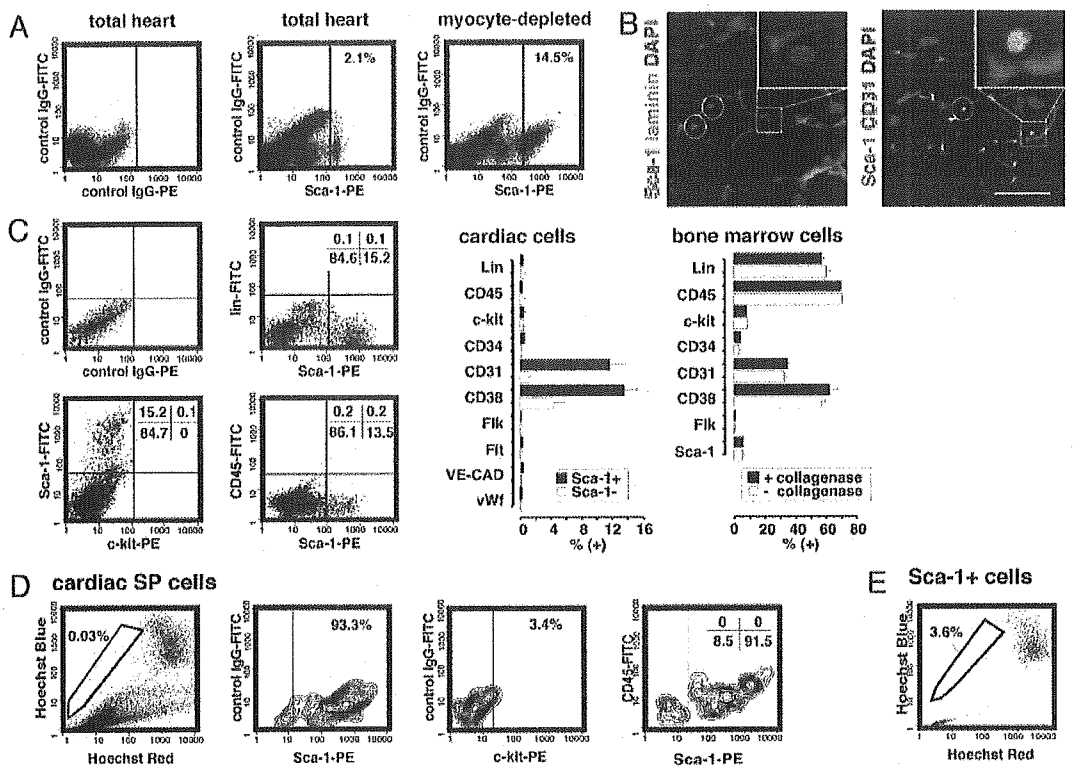

Fig. 1. Isolation of Sca-1$^+$ cells from adult mouse myocardium. (*A*) Sca-1 was analyzed by flow cytometry (MoFlo, Cytomation, Ft. Collins, CO), by using IgG2a + 2b-FITC as the control. (*B*) Immunostaining of adult mouse myocardium for Sca-1, laminin, and CD31. Yellow-orange in the merged images denotes colocalization. Representative cells are highlighted in white and shown at higher magnification (*Insets*). (Bar = 15 μm.) (*C*) Cells were labeled with Sca-1 plus the indicated markers (EPICS XL-MCL, Beckman Coulter). Values in the bar graph denote prevalence in the myocyte-depleted population, e.g., 12% are Sca-1$^+$CD31$^+$. Bone marrow cells ± collagenase are shown (*Right*). (*D*) Cardiac SP cells were identified with Hoechst 33342 (MoFlo, Cytomation). Labeling with Sca-1 vs. c-kit and CD45 is shown as contour plots. (*E*) Enrichment for SP cells in the cardiac Sca-1$^+$ population.

to 5 d after instrumentation, the left anterior descending coronary artery was occluded for 1 h and reperfused for 6 h. Newly isolated Sca-1$^+$ cells (10^6) from *αMHC-Cre* mice or wild-type littermates were then injected in 100 μl of PBS via the right jugular vein. Mice were killed 2 wk later, with comparable survival (62%) in each group.

Histology and Western Blot. Alexa Fluors for antibody conjugation were from Molecular Probes. To localize Sca-1 plus laminin, Alexa Fluor 495-mouse anti-Sca-1 (Pharmingen) was used with rabbit antilaminin (Sigma) then with FITC-goat anti-rabbit IgG (Sigma). To localize Sca-1 plus CD31, Alexa Fluor 495-mouse anti-CD31 (Pharmingen) was used with FITC-Sca-1. To test homing (dye-labeled cells 24 h after i.v. delivery) and stable engraftment to the heart (dye-labeled cells at 2 wk), >120,000 cells were sampled for each condition. Expression of *R26R* without recombination was assessed by using rabbit antibody to neo (NPTII; Agdia, Elkhart, IN). To detect LacZ activation by Cre$^+$ donor cells, myocytes were stained by using mouse anti-β-galactosidase (Sigma) then Texas red-goat anti-mouse IgG (Molecular Probes), and with FITC-mouse antisarcomeric α-actin (Sigma) or rabbit antilaminin (Sigma) then FITC-goat anti-rabbit IgG (Sigma). To elucidate the prevalence of fusion more precisely, myocardium was triply stained for Cre, neo, and LacZ by using Alexa Fluor 488-mouse anti-Cre (Babco, Richmond, CA); rabbit antibody to neo or laminin, and Alexa Fluor 647-goat anti-rabbit IgG; and Alexa Fluor 594- or 647-mouse anti-β-galactosidase (Fig. 4 *F*, *H*, and *I*). Mouse antibodies to sarcomeric α-actin and cardiac troponin I were conjugated with Alexa Fluor 594 and mouse anticonnexin-43 (Sigma) with Alexa Fluor 647. Mitotic phosphorylation of histone H3 was detected by using rabbit antibody to the serine-10 phosphoepitope (Upstate Biotechnology, Lake Placid, NY) then Alexa Fluor 647-goat anti-rabbit IgG. Irrelevant mouse and rabbit antibodies conjugated with each fluor were the negative controls. Nuclei were counterstained with 4′, 6-diamidino-2-phenylindole. Immunostaining was visualized by confocal microscopy (Zeiss LSM 510). Western blotting for neo was performed by using antibody to neo vs. total actin and enhanced chemiluminescence reagents (Amersham Pharmacia Biotech).

Statistical Analysis. Data (mean ± SE) were analyzed by ANOVA and Scheffé's test, by using a significance level of $P < 0.05$.

Results

Isolation of Sca-1$^+$ Cells from Adult Mouse Myocardium. In adult mouse hearts, cardiomyocytes comprise 20–30% of the total population, the remainder including fibroblasts, vascular smooth muscle, and endothelium (28). We isolated a "myocyte-depleted" fraction of adult cardiac cells using collagenase under conditions lethal for most adult ventricular myocytes, then analyzed the cells by flow cytometry for stem cell markers including Sca-1 and c-kit. Approximately 14–17% of the cells expressed Sca-1 (increased 7-fold, compared with total cardiac cells; Fig. 1*A*). As in skeletal muscle (29), cardiac Sca-1$^+$ cells were small interstitial cells adjacent to the basal lamina, typically coexpressing platelet–endothelial cell adhesion molecules (CD31) and in proximity with endothelial Sca-1$^-$ CD31$^+$ cells (Fig. 1*B*).

Cardiac Sca-1$^+$ cells lacked blood cell lineage markers (CD4,

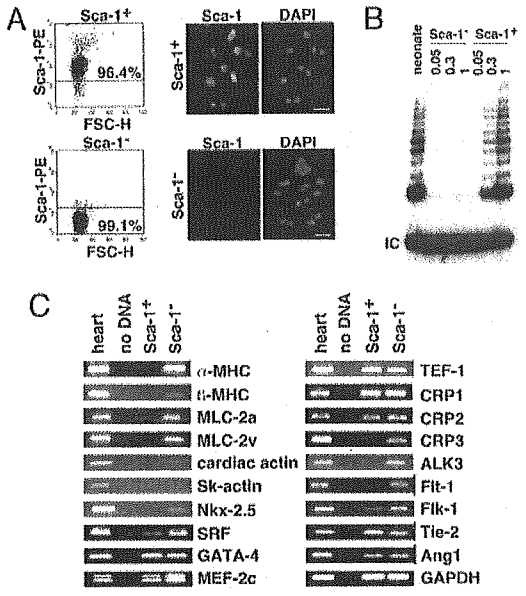

Fig. 2. Purification and culture of cardiac Sca-1$^+$ cells. Purity of cardiac Sca-1$^+$ and -1$^-$ cells after magnetic enrichment. (*A Left*) Flow cytometry. FSC-H, forward-angle light scatter. (*Right*) Immunostaining. (*B*) Telomerase activity (30) was detected in cardiac Sca-1$^+$ cells but not Sca-1$^-$ cells. Numbers above each lane indicate the amount of adult lysate, relative to neonatal mouse heart ("neonate"). (*C*) RT-PCR analysis of cardiac Sca-1$^+$ and -1$^-$ cells vs. adult mouse heart. (Bar in *A* = 5 μm).

CD8, B220, Gr-1, Mac-1, and TER119), c-kit, Flt-1, Flk-1, vascular endothelial-cadherin, von Willebrand factor, and hematopoietic stem cell markers CD45 and -34 (Fig. 1*C*). These features argue against a hematopoietic progenitor cell, endothelial progenitor cell, or mature endothelial phenotype. Levels of markers in bone marrow cells were not diminished by collagenase (Fig. 1*C Right*), excluding spurious effects of enzymatic digestion. Most cardiac Sca-1$^+$ cells express CD31 or its receptor CD38, implicated in cell–cell binding (Fig. 1 *B* and *C*). Conversely, only 1 in 150,000 peripheral blood cells had this phenotype (Sca-1$^+$, lin$^-$, CD45$^-$, CD31$^+$ CD38$^+$; not shown).

By efflux of Hoechst dye 33342, 0.03% of cardiac cells possess the properties of side population (SP) cells (Fig. 1*D*), which are enriched for long-term self renewal in other tissues; their prevalence even in bone marrow is only 0.05% (2, 21, 29). Cardiac SP cells are >93% Sca-1$^+$, differ from marrow SP cells by typically lacking CD45 and c-kit (Fig. 1*D*), and are enriched 100-fold in the Sca-1+ population (Fig. 1*E*).

Cardiac Sca-1$^+$ Cells Express Most Cardiogenic Transcription Factors but Not Cardiac Structural Genes. By magnetic separation, we isolated a Sca-1$^+$ fraction (>96% pure, after five or more rounds) and Sca-1$^-$ fraction (>99% pure, even in the flow-through; Fig. 2*A*). Telomerase reverse transcriptase is associated with self-renewal potential, down-regulated in adult myocardium, and sufficient to prolong cardiomyocyte cycling (30). By a telomeric repeat amplification protocol (30), we detected telomerase activity only in Sca-1$^+$ cells from adult heart but not in Sca-1$^-$ cells, at levels similar to neonatal myocardium (Fig. 2*B*).

By RT-PCR (Fig. 2*C*), Sca-1$^+$ cells express none of the following cardiac genes: α- and β*MHC*, *atrial* and *ventricular myosin light chain-2* (*MLC-2a, -2v*); *cardiac* and *skeletal* α*-actin*; and *muscle LIM protein/cysteine-rich protein-3*. Most were detected in Sca-1$^-$ cells, consistent with the presence of some myocytes in the starting "myocyte-depleted" fraction. Sca-1$^+$ cells did not express *Nkx2.5* and had minimal levels of *SRF*. However, other cardiogenic transcription factors were expressed (*GATA-4*, *MEF-2C*, and *TEF-1*), as in marrow stromal cells with cardiogenic potential (1). Consistent with the lack of Flt-1 and Flk-1 by flow cytometry (Fig. 1*C*), little or no expression was seen by RT-PCR (Fig. 2*C*). Sca-1$^-$ cells did express *Tie-2* and *angiopoietin-1* (*Ang1*), ostensibly vascular markers found also in marrow SP cells (2).

Microarray profiling (Table 1) was concordant with these results, extending the cardiac structural genes that are not expressed in cardiac Sca-1$^+$ cells, and adding Bop and popeye-3 as cardiogenic transcription factors that are absent. Neither CD45, CD34, c-kit, nor Flt-1 was detected, nor the hematopoietic stem cell transcription factors Lmo2, GATA2, and Tal1/Scl. Adult cardiac Sca-1$^+$ cells were enriched, as expected, for diverse cell cycle mediators, growth factors, cytokines, and chemokines. Sca-1$^+$ cells also express multiple transcriptional repressors (DNA methyltransferase-1, histone deacetylase-1, the Notch

Table 1. Expression profiling of adult cardiac Sca-1$^+$ cells vs. cardiomyocytes

Transcripts detected in purified adult cardiac myocytes but not cardiac Sca-1$^+$ cells*
- Sarcomeric proteins: Acta1, Actc1, Mybpc3, Myhca, Myhcb, Mylc, Mylc2a, Mylpc, Myom1, Myom2, Tncc, Tnni3, Tnnt1
- Transcription factors: Bop, Csrp3, Nkx2–5, Pop 3
- Growth factors: Fgf1
- Metabolism: Acas2, Adss1, Art1, Ckmt2, Ckmm, Cox6a2, Cox7a1, Cox8b, Crat, Cyp4b1, Fabp3, Facl2, Mb, Pgam2, Pygm, Slc2a4
- Ion transport: Atp1a2, Cacna1s, Casq2, Kcnq1, Kcnj8, Ryr2
- Other: Cdh13, Ldb3, Nppb, Sgca, Sgog

Transcripts detected in cardiac Sca-1$^+$ cells but not purified adult cardiac myocytes†
- Growth factors, cytokines, receptors: Adm, Bmp1, Csf1, Crlf1, Fgfr1, Figf, Frzb, Fzd2, Inhba, Inhbb, Igf1, Igfbp2, Igfbp4, Il4ra, Il6, Pdgfra, Sfrp1, Scya2, Scya7, Scya9, Scyb5, Sdf1, Tgfb2, Tnfrsf6, Vegfc, Wisp1, Wisp2
- Transcription factors: Aebp1, Csrp, Csrp2, Dnmt1, Edr2, Foxc2, Hey1, Hdac1, Madh7, Ndn, Nmyc1, Odz3, Pias3, runx1, runx2, Tcf21, Twist, ZBP-99
- Cell cycle: Cdc2a, Cks1, Ccnb1-rs1, Ccnc, Ccne2, Prim2, Mki67, MCM7, Rab6kifl, Rev3l, Rrm1, Tyms, Top2a
- Adhesion, recognition: Anxa1, Npnt, Nid2, Ptx3, Tm4sf6, Vcam1
- Signal transduction: Borg4, Cask, Ect2, Eif1a, Lasp1, Map3k6, Map3k8, Pscd3, Sphk1, Stk6, Stk18, Tc101, Wrch1
- Extracellular matrix: Adam9, Mmp3, Col1a1, Col1a2, Col3a1, Col4a5, Col5a, Col5a2, Col8a1, Lox, Spp1, Timp, Tnc

*Two hundred seventy-five transcripts were detected in adult cardiac myocytes but not adult cardiac Sca-1$^+$ cells, of which relevant transcripts with an 8-fold or more change in signal intensity are shown. Others include 35 ESTs, 37 RIKEN cDNAs, and 11 unannotated mRNAs.

†Eight hundred sixteen transcripts were detected in adult cardiac Sca-1$^+$ cells but not adult heart, of which relevant transcripts with an 8-fold or more change in signal intensity are shown. Others include 116 ESTs, 154 RIKEN cDNAs, and 28 unannotated mRNAs.

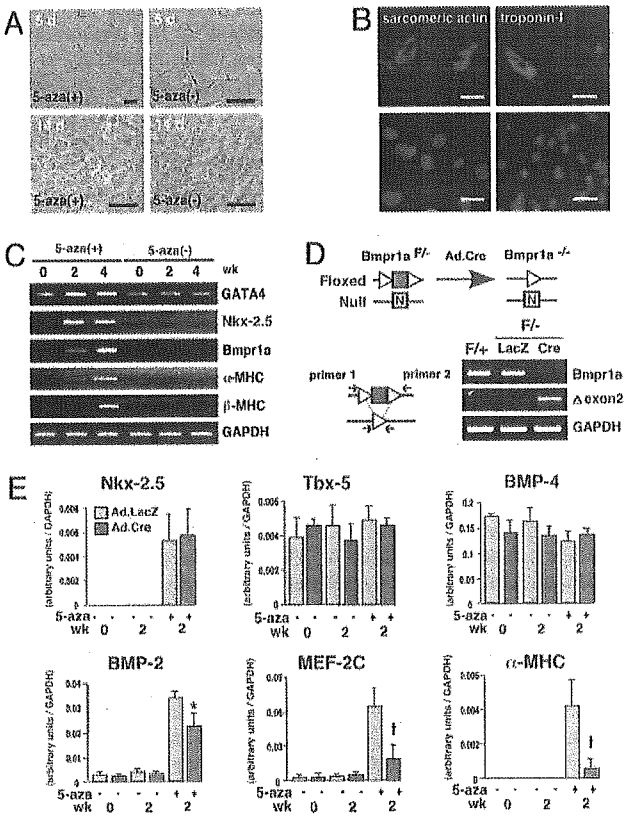

Fig. 3. *In vitro* differentiation of cardiac Sca-1$^+$ cells is induced by 5-aza and depends on a BMP receptor. (*A*) Phase-contrast microscopy. (*B*) Induction of sarcomeric α-actin and cardiac troponin I by using 5-aza, shown by immunostaining (4 wk). Differentiated cells (red) are found in the monolayer with 4′,6-diamidino-2-phenylindole (blue). (*C*) Induction of *Nkx-2.5*, *Bmpr1a*, and cardiac *MHC* genes using 5-aza, shown by RT-PCR. (*D*) Cartoon of the floxed and null *Bmpr1a* alleles at exon 2. (*Bottom Right*) Excision of exon 2 after viral delivery of Cre, shown by PCR. (*E*) Cardiac Sca-1$^+$ cells from Bmpr1a$^{F/-}$ mice were subjected to viral gene transfer, differentiated with 5-aza, and analyzed by quantitative real-time-PCR. White, β-gal; black, Cre. *, $P < 0.05$; †, $P < 0.01$; $n = 6$. [Bars = 20 μm (*A*) and 10 μm (*B*).]

effector Hes1, and Groucho-binding proteins runx1 and -2), as found in adult and embryonic stem cells (31). Absence of Oct-4 and UTF-1, by microarray profiling, was confirmed by RT-PCR.

***In Vitro* Differentiation of Cardiac Sca-1$^+$ Cells.** The cytosine analog 5-aza can induce cardiac differentiation by marrow stromal cells (1), suggesting its possible utility here. Cells treated with 3 μM of 5-aza for 3 d, starting 3 d after plating, gradually developed multicellular spherical structures (Fig. 3*A*), then flattened after 2 wk. Immunostaining at 4 wk confirmed the induction of sarcomeric α-actin (4.6 ± 1.2%) and cardiac troponin-I (2.8 ± 0.9%) in treated cells (Fig. 3*B*) but not untreated ones (not shown). *Nkx-2.5*, *αMHC*, *βMHC*, and type 1*A* receptor for bone morphogenetic proteins (*Bmpr1a*) that are involved in heart development (25), were highly induced by 5-aza (Fig. 3*C*); all but *βMHC* were apparent at 2 wk. None was expressed in the absence of 5-aza or in cells treated with 1% DMSO (not shown).

Although myocyte-restricted deletion of *Bmpr1a* disrupts cardiac organogenesis, lethality at gastrulation in homozygous-null mice obscures the gene's role in cardiac specification (25), and differing mechanisms mediate cardiac fate, depending on the progenitors examined (4, 23). Therefore, Sca-1$^+$ cells from *Bmpr1a*$^{F/-}$ hearts (containing one loxP-flanked and one null allele) were exposed to adenovirus encoding LacZ vs. Cre (Fig. 3*D*). Disruption of *Bmpr1a* by Cre was confirmed by PCR (Fig. 3*D*) and differentiation was compared by using quantitative real-time PCR (Fig. 3*E*). Neither *Tbx5* nor *BMP-4* required 5-aza for expression, and their expression was unchanged in the absence of *Bmpr1a*. By contrast, deletion of *Bmpr1a* significantly impaired the induction of *BMP-2*, *MEF-2C*, and, especially, *α-MHC*. Of the genes investigated, only *Nkx-2.5* was induced by 5-aza yet unaffected by disruption of *Bmpr1a*.

A Cre/Lox Donor/Reporter System Demonstrates Homing, Differentiation, and Fusion of Cardiac Sca-1$^+$ Cells in Injured Myocardium. In proof-of-concept studies to explore the feasibility of homing and stable engraftment to the heart, we labeled cardiac Sca-1$^+$ cells with the membrane dye PKH2-GL and injected cells i.v. after ischemia/reperfusion injury (Fig. 4 *A* and *D*). Donor cells were detected in myocardium within 24 h by epifluorescence microscopy (mean, 0.8 ± 0.05% of total left ventricular cells) but were absent from the infarct itself; uninfarcted regions, lung, liver, kidney, and control mice received Sca-1$^+$ cells without infarction. As with marrow-derived mesenchymal stem cells (32, 33), cardiac Sca-1$^+$ cells were also detected in the spleen (not shown). Persistence of the grafted cells in myocardium at 2 wk ("engraftment") was confirmed in 10 of 14 mice (5.1 ± 1.1%, suggesting proliferation in the interim) and induction of sarcomeric α-actin confirmed in >60% of dye-labeled cells. Donor-derived sarcomeric actin-positive cells were abundant in the infarct border zone (18.1 ± 4.4%) but there were 200-fold fewer after injecting Sca-1$^-$ cells (0.08 ± 0.002%).

Next, we used a Cre/Lox donor/recipient pair as a more conclusive genetic tag of cell identity and a means to test the issue of cell fusion (Fig. 4 *A–C* and *E–I*). Here, differentiation of donor cells is reflected by induction of *αMHC-Cre* and fusion between donor and host cells by activation of *LacZ*. *αMHC* is a late but stringent criterion of cardiac differentiation, and no promiscuous expression is seen with *αMHC-Cre* (25, 34). Newly isolated cardiac *Sca*I$^+$ cells from *αMHC-Cre* mice do not express Cre (Fig. 4*B*), as anticipated from their lack of endogenous *αMHC* (Figs. 2*C* and 3*C*). To monitor *R26R* expression in adult hearts, we first stained for neo, which provides the LoxP-flanked "stop" signal upstream from *LacZ* and should be present in all *R26R* cells lacking Cre. *R26R* mice express neo by Western blotting, wild-type C57BL/6 mice do not express neo, and *R26R* mice stain homogenously for neo throughout myocardium even in the infarct border zone (Fig. 4 *C* and *E*).

Two weeks after injury and infusion of undifferentiated *αMHC-Cre* Sca-1$^+$ cells, nuclear-localized Cre protein was detected specifically in the infarct border zone (Fig. 4 *F–I*). The prevalence of Cre$^+$ nuclei in the left ventricle was ≈3% ($n = 3$; 75,000 sampled), engraftment 150-fold greater than reported for endogenous marrow-derived SP cells (35). Cre$^+$ cells were localized almost exclusively to anterolateral myocardium, and the region was subjected to infarction (Fig. 4*G*). Coexpression of Cre and LacZ was readily apparent in half the Cre$^+$ cells, as evidence of chimerism (Fig. 4*G*). Injection of nontransgenic cardiac Sca-1$^+$ cells lacking *αMHC-Cre* did not produce Cre protein or activate *LacZ* (Fig. 4*F Left*). By immunostaining for LacZ plus sarcomeric α-actin or laminin, *LacZ* activation was confined to myocytes (Fig. 4 *F* and *H*, and data not shown).

We do not know whether fusion precedes differentiation or vice versa. However, roughly half the cells expressing *αMHC-Cre* did not express LacZ (Fig. 4 *F–I*). These Cre$^+$LacZ$^-$ cells could indicate differentiation autonomous of fusion (bona fide cardiopoiesis) or, alternatively, fused cells with incomplete penetrance for recombination. By triple staining for neo plus LacZ and Cre, fused cells without recombination were identifiable sporadically but minute in prevalence and did not contribute significantly to the Cre$^+$ population (Fig. 4*F Right*). Regardless

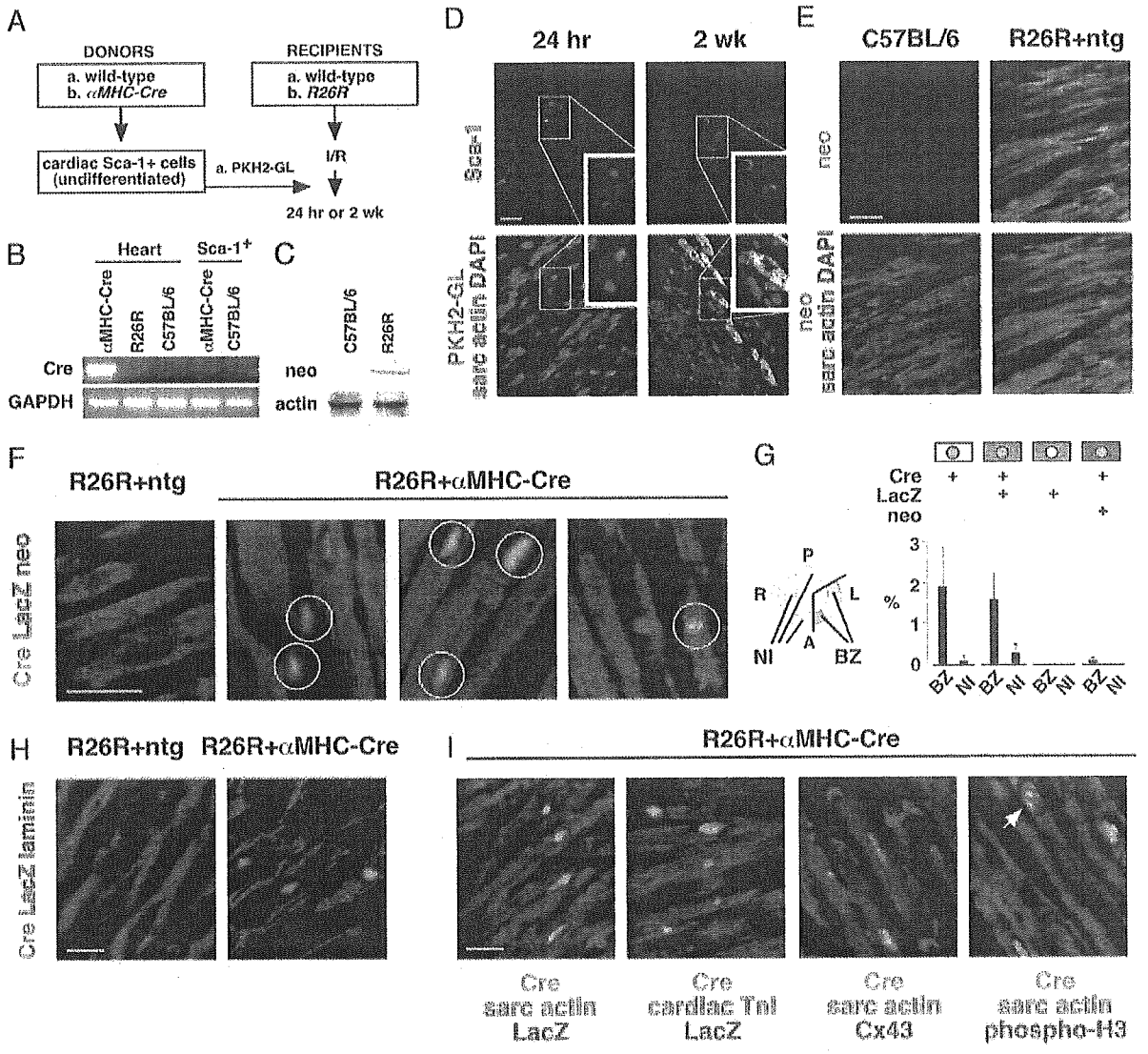

Fig. 4. Homing, differentiation, and fusion of donor cardiac Sca-1$^+$ cells in host myocardium. Diagram of the dye-labeling (*A*) and Cre/Lox (*B*) donor/recipient strategies. (*B*) RT-PCR analysis showing lack of Cre expression in newly isolated cardiac Sca-1$^+$ cells from *αMHC-Cre* mice. (*C*) Western blot showing expression of neo in *R26R* mice. (*D*) Homing of dye-labeled cardiac Sca-1$^+$ cells at 24 h (*Left*) and engraftment at 2 wk (*Right*). (*E*) Neo (FITC; yellow in merged image) was ubiquitously expressed in *R26R* adult ventricular myocardium. (*D* and *E*) Identical fields are shown, *Upper* and *Lower*. Cardiomyocytes were identified by sarcomeric α-actin (Texas red) and nuclei with 4′,6-diamidino-2-phenylindole. (*F–I*) Animals were analyzed by confocal microscopy 2 wk after ischemia-reperfusion injury and infusion of *Sca1*$^+$ cells. (*F*) Neo (blue) was ubiquitously expressed in adult ventricular myocardium of *R26R* mice. Grafted Sca-1$^+$ cells from *αMHC-Cre* mice activate cardiomyocyte-specific *Cre*, and recombination of *R26R*. Cre protein (green) was localized to nuclei. Three phenotypes resulted. Unfused donor-derived cells express neither neo nor LacZ (circled in column 2). Fusion with host *R26R* myocardium typically results in LacZ$^+$ muscle cells (red; circled in column 3). Fused cells without recombination were detected very rarely (circled in column 4). (*G*) Mean ± SE for donor-derived myocytes with (Cre$^+$ LacZ$^+$ neo$^-$; Cre$^+$ LacZ$^-$ neo$^+$) and without (Cre$^+$ LacZ$^-$ neo$^-$) fusion after grafting. BZ, infarct border zone in anterolateral (A, L) myocardium; NI, noninfarcted control regions; P, posterior wall; R, right ventricle, interventricular septum. (*H*) Delineation of Cre$^+$ cells by laminin. (*I*) All Cre$^+$ cells coexpressed sarcomeric α-actin, cardiac troponin I, and Cx43. Mitotic phosphorylation of histone H3 2 wk after grafting was seen almost exclusively in donor-derived Cre$^+$ myocytes. Arrow, Cre$^+$ phospho-H3$^+$ cardiomyocyte nuclei (blue-green in merged image). (Bar = 20 μm.) ntg, nontransgenic.

of the presence or absence of fusion, all donor-derived differentiated (Cre$^+$) cells expressed sarcomeric α-actin, cardiac troponin I, and connexin-43 (Fig. 4*I*).

Assayed 2 wk after cell grafting, 5% of Cre$^+$ sarcomeric actin$^+$ cells (41/816) stained for the serine-10 phosphorylation of histone H3, a marker of mitotic Cdc2 activity (30), vs. only 0.00004% of Cre$^-$ cardiomyocytes (1/24,000; Fig. 4*I*).

Discussion

The inexorability of heart failure has prompted studies of interventions to supplant cardiac muscle cell number. A foundation for such efforts is to know what cells can be coaxed into a cardiac fate and how this transition is governed. By using cardiac-specific Cre to denote donor cell identity and differentiation *in situ*, we provide genetic evidence that cardiac muscle progenitors can be isolated from the adult heart. However, the frequent occurrence of LacZ$^+$ chimeric cells, *in vivo* in the absence of selection pressure, provides a further cautionary note in the interpretation of adult cell plasticity (15, 16). Cell fusion is typical of skeletal muscle myoblasts forming myotubes, but binucleation in postnatal ventricular myocytes occurs by uncoupling karyokinesis from cytokinesis. Cardiac

cell fusion does not occur ordinarily, and diffusion through gap junctions does not occur for molecules the size of Cre or LacZ protein.

Distinct from hematopoietic stem cells (based on CD45, CD34, c-kit, Lmo2, GATA2, and Tal1/Scl) and endothelial progenitor cells (based on CD45, CD34, Flk-1, and Flt-1), cardiogenic Sca-1$^+$ cells perhaps best resemble the highly myogenic cells in skeletal muscle that are Sca-1$^+$ but CD45$^-$, CD34$^-$, and c-kit$^-$ (22); these differ from muscle "satellite" cells (Sca-1$^-$, CD34$^+$) (11), muscle-derived hematopoietic stem cells (CD45$^+$) (22), and multipotential muscle cells (Sca-1$^+$, CD34$^+$) (36). Conceptually, the presence of Tie-2, Ang-1, and CD31 in the absence of all of the markers above might denote a primitive hemangioblast or its precursor. Surface labeling like that of cardiac Sca-1$^+$ cells also was reported for multipotent adult progenitor cells from bone marrow, but these home to normal liver and lung, lack mesoderm transcription factors, and express minimal Sca-1 (33). Our data concur with the finding of SP cells in adult mouse myocardium that lack CD45 and hematopoietic potential (37). *In vitro*, cardiac myogenesis by heart-derived Sca-1$^+$ cells depends at least in part on *Bmpr1a*, which may signify a useful pathway to promote their differentiation into cardiac muscle *in vivo*.

Because we used *αMHC-Cre* expression as the definitive marker of donor cell identity, we confine our analysis here to donor-derived cardiomyocytes. Alternative lineage markers, clonal studies, and other methods will be needed to pinpoint the cells' fates and origin. If progenitor cells are assumed conservatively to be just a small proportion of the Sca-1$^+$ cells, even minute subpopulations like SP cells could be essential to the phenotype observed. Knowledge of the cells' source and migration during development could also be instrumental to resolving a seeming paradox: although isolated from the heart, exogenous cardiac Sca-1$^+$ cells are not recruited there in the absence of injury.

Adult ventricular myocytes are refractory to cell cycle reentry for reasons that include their lack of telomerase activity (30). Cardiac Sca-1$^+$ cells offer auspicious properties for cardiac repair, including high levels of telomerase, homing to injured myocardium, and dependence on the well defined BMP pathway. We emphasize the incompleteness of myocardial repair as executed by all endogenous mechanisms collectively, including whatever progenitors exist intrinsic and extrinsic to the heart. Although endogenous Sca-1$^+$ cells are present in the heart, engrafted ones accounted for virtually all of the cycling myocytes 14 d after infarction. Thus, there exists both need and opportunity to augment cardiac Sca-1$^+$ cell number or function.

We thank M. Goodell, R. Schwartz, D. Chang, M. Majesky, and K. Hirschi for suggestions, and M. Mancini and the Baylor Integrated Microscopy Core for confocal microscopy. This work was supported by National Institutes of Health grants (to M.D.S. and M.L.E.) and the M. D. Anderson Foundation Professorship (to M.D.S.).

1. Makino, S., Fukuda, K., Miyoshi, S., Konishi, F., Kodama, H., Pan, J., Sano, M., Takahashi, T., Hori, S., Abe, H., *et al.* (1999) *J. Clin. Invest.* **103,** 697–705.
2. Jackson, K. A., Majka, S. M., Wang, H., Pocius, J., Hartley, C. J., Majesky, M. W., Entman, M. L., Michael, L. H., Hirschi, K. K. & Goodell, M. A. (2001) *J. Clin. Invest.* **107,** 1395–1402.
3. Orlic, D., Kajstura, J., Chimenti, S., Jakoniuk, I., Anderson, S. M., Li, B., Pickel, J., McKay, R., Nadal-Ginard, B., Bodine, D. M., *et al.* (2001) *Nature* **410,** 701–705.
4. Condorelli, G., Borello, U., De Angelis, L., Latronico, M., Sirabella, D., Coletta, M., Galli, R., Balconi, G., Follenzi, A., Frati, G., *et al.* (2001) *Proc. Natl. Acad. Sci. USA* **98,** 10733–10738.
5. Badorff, C., Brandes, R. P., Popp, R., Rupp, S., Urbich, C., Aicher, A., Fleming, I., Busse, R., Zeiher, A. M. & Dimmeler, S. (2003) *Circulation* **107,** 1024–1032.
6. Beltrami, A. P., Urbanek, K., Kajstura, J., Yan, S. M., Finato, N., Bussani, R., Nadal-Ginard, B., Silvestri, F., Leri, A., Beltrami, C. A., *et al.* (2001) *N. Engl. J. Med.* **344,** 1750–1757.
7. Castro, R. F., Jackson, K. A., Goodell, M. A., Robertson, C. S., Liu, H. & Shine, H. D. (2002) *Science* **297,** 1299.
8. Wagers, A. J., Sherwood, R. I., Christensen, J. L. & Weissman, I. L. (2002) *Science* **297,** 2256–2259.
9. Anderson, D. J., Gage, F. H. & Weissman, I. L. (2001) *Nat. Med.* **7,** 393–395.
10. Blau, H. M., Brazelton, T. R. & Weimann, J. M. (2001) *Cell* **105,** 829–841.
11. Seale, P., Asakura, A. & Rudnicki, M. A. (2001) *Dev. Cell* **1,** 333–342.
12. Kamihata, H., Matsubara, H., Nishiue, T., Fujiyama, S., Tsutsumi, Y., Ozono, R., Masaki, H., Mori, Y., Iba, O., Tateishi, E., *et al.* (2001) *Circulation* **104,** 1046–1052.
13. Orlic, D., Kajstura, J., Chimenti, S., Limana, F., Jakoniuk, I., Quaini, F., Nadal-Ginard, B., Bodine, D. M., Leri, A. & Anversa, P. (2001) *Proc. Natl. Acad. Sci. USA* **98,** 10344–10349.
14. Glaser, R., Lu, M. M., Narula, N. & Epstein, J. A. (2002) *Circulation* **106,** 17–19.
15. Vassilopoulos, G., Wang, P. R. & Russell, D. W. (2003) *Nature* **422,** 901–904.
16. Wang, X., Willenbring, H., Akkari, Y., Torimaru, Y., Foster, M., Al-Dhalimy, M., Lagasse, E., Finegold, M., Olson, S. & Grompe, M. (2003) *Nature* **422,** 897–901.
17. Strauer, B. E., Brehm, M., Zeus, T., Kostering, M., Hernandez, A., Sorg, R. V., Kogler, G. & Wernet, P. (2002) *Circulation* **106,** 1913–1918.
18. Assmus, B., Schachinger, V., Teupe, C., Britten, M., Lehmann, R., Dobert, N., Grunwald, F., Aicher, A., Urbich, C., Martin, H., *et al.* (2002) *Circulation* **106,** 3009–3017.
19. Menasché, P., Hagege, A. A., Vilquin, J.-T., Desnos, M., Abergel, E., Pouzet, B., Bel, A., Saratenau, S., Scorsin, M., Schwartz, K., *et al.* (2003) *J. Am. Coll. Cardiol.* **41,** 1078–1083.
20. Zhou, Y. Y., Wang, S. Q., Zhu, W. Z., Chruscinski, A., Kobilka, B. K., Ziman, B., Wang, S., Lakatta, E. G., Cheng, H. & Xiao, R. P. (2000) *Am. J. Physiol.* **279,** H429–H436.
21. Goodell, M. A., Brose, K., Paradis, G., Conner, A. S. & Mulligan, R. C. (1996) *J. Exp. Med.* **183,** 1797–1806.
22. McKinney-Freeman, S. L., Jackson, K. A., Camargo, F. D., Ferrari, G., Mavilio, F. & Goodell, M. A. (2002) *Proc. Natl. Acad. Sci. USA* **99,** 1341–1346.
23. Monzen, K., Shiojima, I., Hiroi, Y., Kudoh, S., Oka, T., Takimoto, E., Hayashi, D., Hosoda, T., Habara-Ohkubo, A., Nakaoka, T., *et al.* (1999) *Mol. Cell. Biol.* **19,** 7096–7105.
24. Murohara, T., Ikeda, H., Duan, J., Shintani, S., Sasaki, K., Eguchi, H., Onitsuka, I., Matsui, K. & Imaizumi, T. (2000) *J. Clin. Invest.* **105,** 1527–1536.
25. Gaussin, V., Van De Putte, T., Mishina, Y., Hanks, M. C., Zwijsen, A., Huylebroeck, D., Behringer, R. R. & Schneider, M. D. (2002) *Proc. Natl. Acad. Sci. USA* **99,** 2878–2883.
26. Soriano, P. (1999) *Nat. Genet.* **21,** 70–71.
27. Nossuli, T. O., Lakshminarayanan, V., Baumgarten, G., Taffet, G. E., Ballantyne, C. M., Michael, L. H. & Entman, M. L. (2000) *Am. J. Physiol.* **278,** H1049–H1055.
28. Soonpaa, M. H., Kim, K. K., Pajak, L., Franklin, M. & Field, L. J. (1996) *Am. J. Physiol.* **271,** H2183–H2189.
29. Asakura, A., Seale, P., Girgis-Gabardo, A. & Rudnicki, M. A. (2002) *J. Cell Biol.* **159,** 123–134.
30. Oh, H., Taffet, G. E., Youker, K. A., Entman, M. L., Overbeek, P. A., Michael, L. H. & Schneider, M. D. (2001) *Proc. Natl. Acad. Sci. USA* **98,** 10308–10313.
31. Ramalho-Santos, M., Yoon, S. J., Matsuzaki, Y., Mulligan, R. C. & Melton, D. A. (2002) *Science* **298,** 597–600.
32. Toma, C., Pittenger, M. F., Cahill, K. S., Byrne, B. J. & Kessler, P. D. (2002) *Circulation* **105,** 93–98.
33. Jiang, Y., Jahagirdar, B. N., Reinhardt, R. L., Schwartz, R. E., Keene, C. D., Ortiz-Gonzalez, X. R., Reyes, M., Lenvik, T., Lund, T., Blackstad, M., *et al.* (2002) *Nature* **418,** 41–49.
34. Agah, R., Frenkel, P. A., French, B. A., Michael, L. H., Overbeek, P. A. & Schneider, M. D. (1997) *J. Clin. Invest.* **100,** 169–179.
35. Jackson, K. A., Mi, T. & Goodell, M. A. (1999) *Proc. Natl. Acad. Sci. USA* **96,** 14482–14486.
36. Torrente, Y., Tremblay, J. P., Pisati, F., Belicchi, M., Rossi, B., Sironi, M., Fortunato, F., El Fahime, M., D'Angelo, M. G., Caron, N. J., *et al.* (2001) *J. Cell Biol.* **152,** 335–348.
37. Asakura, A. & Rudnicki, M. A. (2002) *Exp. Hematol.* **30,** 1339–1345.